Review article

A perspective on three sustainable hydrogen production technologies with a focus on technology readiness level, cost of production and life cycle environmental impacts

Yunfei Li [a,c], Richen Lin [b,c,*], Richard O'Shea [a,c,**], Vaishali Thaore [a,c], David Wall [a,c], Jerry D. Murphy [a,c]

[a] *MaREI Centre for Energy Climate and Marine, Environmental Research Institute, University College Cork, Cork, T23 XE10, Ireland*
[b] *Key Laboratory of Energy Thermal Conversion and Control of Ministry of Education, School of Energy and Environment, Southeast University, Nanjing, 210096, China*
[c] *Civil, Structural and Environmental Engineering, School of Engineering and Architecture, University College Cork, Cork, T12 YN60, Ireland*

ABSTRACT

Hydrogen will play an indispensable role as both an energy vector and as a molecule in essential products in the transition to climate neutrality. However, the optimal sustainable hydrogen production system is not definitive due to challenges in energy conversion efficiency, economic cost, and associated marginal abatement cost. This review summarises and contrasts different sustainable hydrogen production technologies including for their development, potential for improvement, barriers to large-scale industrial application, capital and operating cost, and life-cycle environmental impact. Polymer electrolyte membrane water electrolysis technology shows significant potential for large-scale application in the near-term, with a higher technology readiness level (expected to be 9 by 2030) and a levelized cost of hydrogen expected to be 4.15–6 €/kg H_2 in 2030; this equates to a 50% decrease as compared to 2020. The four-step copper-chlorine (Cu–Cl) water thermochemical cycle can perform better in terms of life cycle environmental impact than the three- and five-step Cu–Cl cycle, however, due to system complexity and high capital expenditure, the thermochemical cycle is more suitable for long-term application should the technology develop. Biological conversion technologies (such as photo/dark fermentation) are at a lower technology readiness level, and the system efficiency of some of these pathways such as biophotolysis is low (less than 10%). Biomass gasification may be a more mature technology than some biological conversion pathways owing to its higher system efficiency (40%–50%). Biological conversion systems also have higher costs and as such require significant development to be comparable to hydrogen produced via electrolysis.

1. Introduction

Developing renewable energy systems is strategically imperative for the energy transition. The range of technologies available has different characteristics, advantages, disadvantages, environmental impacts and levels of sustainability. It is essential to optimise the

---

* Corresponding author. Southeast University, Nanjing 210096, China.
** Corresponding author. University College Cork, Cork T23 XE10, Ireland.
E-mail addresses: richenlin@seu.edu.cn (R. Lin), richard.oshea@ucc.ie (R. O'Shea).

List of abbreviations including units and nomenclature

ADP-a	Abiotic resource depletion potential
ADP	Adenosine diphosphate
AE	Alkaline electrolysis
AEC	Alkaline electrolysis cell
AP	Acidification potential
ATP	Adenosine triphosphate
CAPEX	Capital expenditures
CCS	Carbon capture and storage
CEPCI	Chemical engineering plant cost index
Cu–Cl	Copper-chlorine cycle
DC	Direct current
e	Electrons
EED	Electro-electrodialysis
EP	Eutrophication potential
EU	European Union
Fdred	Ferredoxin
Fdox	Flavodoxin
GHG	Greenhouse gas
GWP	Global warming potential
H^+	Hydrogen proton
H_2	Hydrogen
HHV	High heating value
HI	Hydriodic acid
H_2O	Water
H_2SO_4	Sulfuric acid
HT	High temperature
JAEA	Japan Atomic Energy Agency
JRC	Joint Research Centre
LCA	Life cycle assessment
LCOH	Levelized cost of hydrogen
LHV	Low heating value
LT	Low temperature
MoS_2	Molybdenum disulfide
ODP	Ozone depletion potential
O&M	Operation and management
OPEX	Operating expenditures
Pd	Palladium
PEM	Polymer electrolyte membrane
PEMEC	Polymer electrolyte membrane electrolysis cell
PIK	Potsdam Institute for Climate Impact Research
Pt	Platinum
PSI	Photosystem
SO_2	Sulfur dioxide
SOE	Solid oxide electrolysis
SOEC	Solid oxide electrolysis cell
S–I	Sulfur-iodine cycle
TRL	Technology readiness level
Mt/a	Million tonnes per year
V	Voltage
A	Ampere
$A\ cm^{-2}$	Ampere per square centimetre
m^2	Square meter
K	Kelvin
€/a	Euro per year
€/kWh	Euro per kilowatt hour
€/kg	Euro per kilogram
Wt	Weight
$m^3H_2h^{-1}$	Cubic meter hydrogen per hour

sustainability of such renewable energy technologies by protecting the environment, minimising climate impact, and optimizing sustainable economic and social development. Hydrogen (H_2) is a versatile energy carrier with the potential to be utilized as an alternative to fossil fuels in a compressed form, such as for use directly in fuel cells and in hard-to-abate sectors such as heavy-duty vehicle transportation.

In the last five years, interest in hydrogen has soared: many organisations, regions, and companies consider hydrogen as indispensable to achieving the Paris Agreement's objective of maintaining global warming below 2 °C and closer to 1.5 °C [1]. The different techniques for sustainable hydrogen production, end-use technologies, and applications define the technological boundaries of the hydrogen economy. Current greenhouse gas (GHG) emissions from the reforming of fossil fuels to produce hydrogen account for 2% of global CO_2-eq emissions, roughly 900 Mt CO_2-eq annually [2]. Scaling up the hydrogen economy may be problematic if GHG-emitting technologies continue to be used to produce hydrogen. It is critical that hydrogen should be produced with as low a GHG footprint as feasible and at an attractive cost comparable to fossil-derived hydrogen. To accomplish the decarbonisation of hydrogen production technologies, several obstacles must be overcome, including for electricity sources, sustainable hydrogen infrastructure, and social acceptance.

In the European Union's (EU) hydrogen strategy, the target for sustainable hydrogen production from electrolysis (from a base of 100 Megawatt (MW) in 2021) is 6 Gigawatt (GW) by 2024; this is equivalent to an annual hydrogen yield of c. 1.6 million tonnes (Mt H_2/a). The target for 2030 is 40 GW, corresponding to 10.6 Mt H_2/a [3]. However, natural gas steam reforming (grey hydrogen) accounts for 48% of current EU hydrogen production, while oil reforming and coal gasification produce 30% and 18% respectively; sustainable hydrogen only accounts for 4% of the total [4–6]. Even though the current hydrogen output in the EU (from all sources) is approximately 9.8 Mt/a [7], sustainable hydrogen production only accounts for 0.39 Mt/a; this is significantly less than the EU 2030 hydrogen strategy target.

The main sustainable hydrogen production technologies may be sub-divided into three categories whose share of the market may be dictated by specific geopolitical regions: 1. Water electrolysis (such as alkaline, polymer electrolyte membrane, and solid oxide [8]) is likely to be associated with wind and tidal power in temperate oceanic zones (such as west of France, Britain and Ireland) or photovoltaics in sunnier climates (such as sub Saharan Africa) [9]; 2. Water thermochemical cycles (such as copper-chlorine and sulfur-iodine cycle [10]) are more likely to be associated with large nuclear facilities [11]; 3. Biomass-based hydrogen production (such as biomass gasification and biological conversion [12]) is more likely in well forested areas (potentially linked with paper and pulp industries) such as Canada and Scandinavia [13].

Sustainable hydrogen infrastructure must be addressed for large-scale development. For example Mijndert et al. [14] highlighted the lack of widespread availability of low cost renewable electricity, especially in regions where non-renewable electricity production dominates as a major barrier; this is of issue for water electrolysis. For biomass based hydrogen production, microalgae (including cyanobacteria and green algae) break down water molecules into oxygen and hydrogen in the presence of carbon dioxide and light in direct biophotolysis process. Vineet et al. [15] found that the barrier for large-scale application of direct biophotolysis technology lies in low photo-hydrogen energy conversion efficiency (less than 10%) and relatively expensive infrastructure. Thus, it is necessary to compare the technical characteristics, advantages and disadvantages of sustainable hydrogen production technologies to identify the difficulties that need to be overcome to allow for future large-scale application. For other issues such as the public acceptability of the hydrogen economy, it is necessary to address and communicate to society at large the evidence-based research on economic and life cycle environmental impacts of hydrogen production technologies. This information must also be synthesised and used to ascertain the carbon footprint and sustainability of sustainable hydrogen production technologies [16].

Taking account of the different issues such as low levels of sustainable hydrogen production, lack of large-scale infrastructure development, immaturity of some technologies, and safety concerns, many existing studies have investigated optimal sustainable hydrogen production technologies. Ishaq [17] modelled water electrolysis sustainable hydrogen production systems based on geothermal energy and solar PV, and compared the system efficiency of water electrolysis and biomass gasification technologies. The study concluded that biomass gasification had higher exergy (49.8%) and energy efficiency (53.6%) than water electrolysis hydrogen production from geothermal power and solar PV. Ahmad et al. [18] conducted techno-economic assessments of sustainable hydrogen production technologies including; dark fermentation (a biological reaction in which fermentative bacteria convert organic compounds to alcohols, acetone, H_2, and CO_2 under anaerobic conditions), photo fermentation, biomass gasification, plasma gasification (a thermal process using plasma to convert biomass into syngas including carbon monoxide and hydrogen) and pyrolysis (thermal decomposition of biomass in the absence of oxygen to biochar, bio-oil and gas). The analysis concluded that dark fermentation performed better from a technical point of view, and the cost of sustainable hydrogen from gasification and fermentation was lower than that from plasma gasification and pyrolysis. Previous studies mainly concentrated on reviewing specific technologies, such as exclusively examining water electrolysis [19] or microbial hydrogen production [20], or limited their comparisons to certain aspects of hydrogen production, such as solely focusing on technical parameters [21] or economic parameters [22]. These studies did not arrive at a definitive answer regarding the optimal hydrogen production technology, taking into account various perspectives such as technical, economic, and environmental aspects.

This study aims to serve as a reference for the large-scale industrial application of hydrogen production technology. To achieve this, technologies attaining a Technology Readiness Level (TRL) between 5 and 9 are encompassed in this paper, signifying their prior validation in practical settings through project-based experimentation. This study aims to provide a comprehensive review of the state-of-the-art of sustainable hydrogen production technologies, including water electrolysis, water thermochemical cycles and biomass-based hydrogen production.

2. Sustainable hydrogen production technologies

2.1. Hydrogen production from water electrolysis

During electrolysis, water undergoes a decomposition reaction under the influence of direct current and produces oxygen and hydrogen simultaneously (Eq. (1)). As hydrogen and oxygen are generated at the anode and cathode separately, they can be collected and stored easily. Electrolysis techniques can be categorized based on the electrolytes employed: alkaline electrolysis (AE); polymer electrolyte membrane (PEM) electrolysis; solid oxide electrolysis (SOE); and anion exchange membrane (AEM) electrolysis [5]. However, the emerging AEM technology is presently confined to a TRL range between 2 and 3 [23]. The existing research dedicated to AEM systems have primarily concentrated on laboratory-scale investigations, primarily centering on the development of electro-catalysts, membrane materials, and operational mechanisms [24]. Consequently, comprehensive data pertaining to AEM system/-system energy efficiency, system construction costs, hydrogen production costs, and environmental impact remain presently unavailable [25].Therefore, the focal point of this paper centres on the remaining three technologies.

$$2H_2O \rightarrow 2H_2 + O_2 \tag{1}$$

2.1.1. Alkaline electrolysis

Since 1920, AE has been in commercial use in the industrial sector. Its advantages include the low capital investment requirement and the low reliance on noble metals and catalysts. Disadvantages include large electricity losses (approximately 40% [26]) and slow start-up speed (which is problematic for association with variable renewable electricity). These disadvantages hinder the large-scale commercial construction and use of AE systems. The typical configuration of AE includes two electrodes (cathode and anode) which are separated by a diaphragm. An hydroxide ion (OH^-) conducting membrane separates the electrolyte compartments associated with the cathode and anode, allowing for the permeation of OH^-, but not the gases produced (H_2 and O_2), H^+, electrons, and K^+/Na^+ [27–29]. Hydrogen gas is formed on the cathode through proton reduction (Eq. (2)) when electricity is applied to water, while hydroxide ions are oxidized with the production of oxygen as a by-product on the anode (Eq. (3)) [30]. Fig. 1 represents the technical principle and layout of the alkaline electrolysis cell (AEC) system.

$$Cathode : 4H_2O + 4e^- \rightarrow 2H_2 + 4OH^- \tag{2}$$

$$Anode : 4OH^- \rightarrow O_2 + 2H_2O + 4e^- \tag{3}$$

For large-scale implementation of AE, a potential technological barrier is efficiency, including system efficiency and electrolysis efficiency. System efficiency differs substantially depending on unit sizes as well as other parameters; nevertheless, a large proportion of the difference in literature can be attributed to the boundaries of the system considered. The whole system efficiency (50%–60%) is approximately 10% lower than the electrolysis efficiency (58%–70%) [26]; this can be attributed to current rectification, purification,
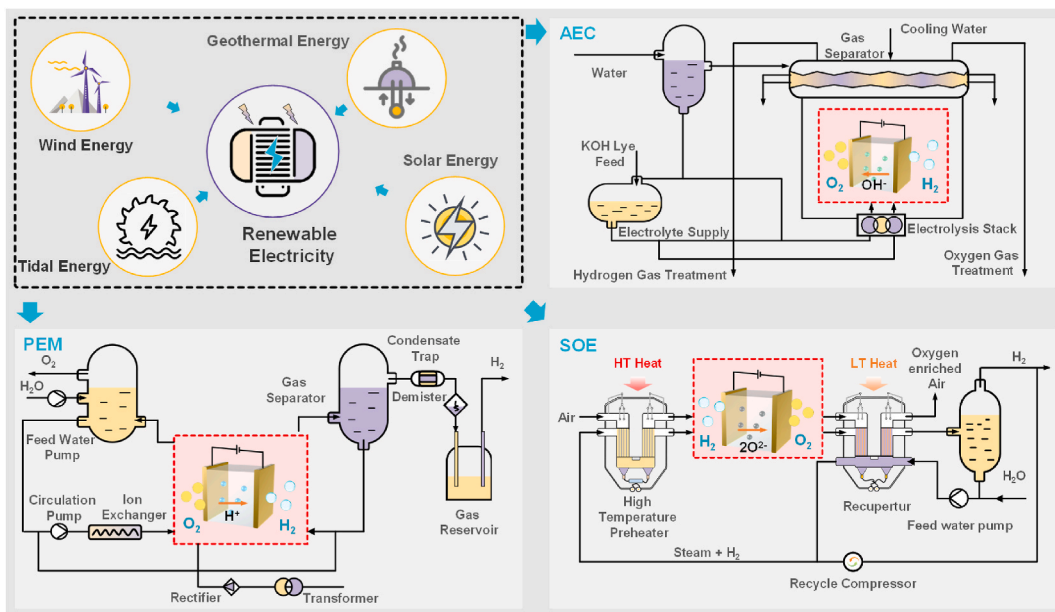

Fig. 1. Simplified layout of three water electrolysis systems for sustainable hydrogen production adapted from Refs. [31,32] (AEC: alkaline electrolysis cell; PEM: polymer electrolyte membrane; SOE: solid oxide electrolysis; HT: high temperature; LT: low temperature; KOH: potassium hydroxide).

compression, and storage. Additionally, system efficiency could be further affected by the electrolysis temperature, plant capacity, and system age. For electrolysis efficiency, many internal and external variables can affect both the electrical behaviour and efficiency of electrolysis cells, including the concentration and purity of the electrolyte, the type and shape of the electrodes, and the cell temperature and pressure [6].

Table 1 compares the main characteristics of AE, PEM, and SOE system. The electrolyte is not consumed in the AE process; it only carries the ionic charges required for water decomposition to oxygen and hydrogen. The majority of studies assessed the use of potassium hydroxide (KOH) in traditional electrolysers at concentrations ranging from 25% to 30% by mass [33]. Studies also examined the use of sodium hydroxide (NaOH) and sodium chloride (NaCl) as electrolytes [34]. Hassen et al. [35] found that the KOH electrolyte is more effective than NaOH at the same concentration and under the same temperature, pressure, and voltage conditions, due to the differences in ionic conductivity and purity.

With regards to electrodes, Slama et al. [36] investigated different types of materials, such as stainless steel, copper, aluminium, bronze, graphite, and lead; the study found stainless steel to be an optimal choice due to its excellent corrosion resistance, low price and electrolytic performance. Despite the high TRL of AE, it presents the disadvantages of low current density and the use of a corrosive electrolyte; this issue should be addressed for more economic and sustainable operation. Of issue when considering electrolysis associated with wind turbines or other variable renewable electricity generators is the cold start time, which is of the order of 60 min.

Table 1

Comparison of different characteristics of water electrolysis-based hydrogen production technologies.

	AEC[a]	PEM[a]	SOE[a]
TRL[a]	9 [51]	8 [51]	6 [51]
Expected TRL 2050	9 [51]	9 [51]	9 [51]
Typical electrolyte	Aqueous potassium hydroxide (20–40 wt% KOH) [52]	Polymer membrane (e.g. Nafion) [38,39]	Yttria Stabilised Zirconia (YSZ) [53]
Anode	Ni or Ni–Co alloys	RuO_2 or IrO_2 [54]	LSM/YSZ [53]
Cathode	Ni or Ni–Mo alloys [38]	Pt or Pt-Pd [54]	Ni/YSZ [53]
Cell voltage (V)	1.8–2.4 [55]	1.8–2.2 [55]	0.7–1.5 [53]
Current density (A cm^{-2})	0.2–0.4 [54]	0.6–2.0 [54]	0.3–2.0 [53]
Cell area (m^2)	<4 [52]	<0.3 [52]	<0.01 [52]
Voltage efficiency (%)	62-82 [55]	67-82 [55]	77-85 [42]
Operating temperature (∘C)	60-80 [39]	50-80 [55]	650-1000 [56]
Operating pressure (bar)	<30 [52]	30-80 [52]	<25 [52]
Production rate ($m^3H_2h^{-1}$)	<760 [52]	<40 [52]	<40 [52]
Stack energy ($kWh_{el}m^3H_2^{-1}$)	4.2–5.9 [55]	4.2–5.5 [55]	>3.2 [52]
System energy ($kWh_{el}m^3H_2^{-1}$)	4.5–6.6 [57]	4.2–6.6 [57]	>3.7
Gas purity (%)	>99.5 [58]	99.99	99.9
Cold-start time (min.)	<60 [59]	<20 [59]	<60
System response	Seconds [52]	Milliseconds [52]	Seconds
Stack lifetime (h)	60,000–90,000 [57]	20,000–60,000 [57]	<10,000 [57]
Capital cost per stack 2020 (€2021/kW)	1000-1200[d] [59]	1860-2320[d] [59]	>2000[d] [59]
Capital cost per stack 2030 (€2021/kW, estimated)	611 [26]	978 [26]	1902 [26]
Stack efficiency (LHV) range 2020 (%)	58–70% [14]	58–65% [14]	81–83% [14]
Stack efficiency (LHV) range 2050 (%, estimated)	61–80% [60]	70–74% [60]	88–90% [60]
Advantages	Long life span	High current density	High system efficiency
	Minimal expense	Compact system layout	Less electricity utilization
	High technology readiness level	Fast response to current change	Expected cost reduction
	Large stack size		Integration with other technologies
Disadvantages	Low current density	Noble metal material requirement	Extraction and utilization of cathodic Lanthanide rare earth elements may cause environmental damage [43]
	Corrosive electrolyte	Short life span	Unstable electrodes
		High membrane expense	Sealing problems
Barriers for large-scale application	Accessibility to low cost and abundant electricity	Accessibility to low cost and abundant electricity	Accessibility to low cost and abundant electricity; immaturity of technology

b: The global share of renewable electricity in total electricity output was approximately 27% at the end of 2019, including 11% produced by wind turbines and solar photovoltaic, which potentially can be used to produce sustainable hydrogen [61].

c: Adequate renewable electricity for large-scale deployment of electrolysis is assumed to be available based on the existing net-zero commitments [62,63].

[a] AEC: alkaline electrolysis cell; GHG: greenhouse gas; LHV: Low heating value; LSM: $La_{0.8}Sr_{0.2}MnO_3$; PEM: polymer electrolyte membrane; SOE: solid oxide electrolysis; TRL: technology readiness level; wt: weight.

[d] Updated capital cost according to Chemical Engineering Plant Cost Index (CEPCI). $CEPCI_{2020} = 596.2$; $CEPCI_{2021} = 708.0$. Calculation formula:

$$cost\ at\ 2021 = cost\ at\ 2020 \cdot \frac{CEPCI\ index\ at\ 2021}{CEPCI\ index\ at\ 2020}\ [64]).$$

2.1.2. Polymer electrolyte membrane electrolysis

General Electric pioneered the PEM electrolysis technology in the 1960s. PEM is less established than AE systems and is primarily employed for small-scale applications [37]. The primary advantages of the PEM technology are associated with the high electricity-to-hydrogen conversion efficiency (approximately 60%), the production of high purity hydrogen (99.99%), as well as the ability to operate flexibly [38]; this is of huge importance for integration with variable renewable electricity generators such as solar and wind. The disadvantages currently include high catalyst (such as Platinum and Palladium) and membrane material expenses, the system's complexity owing to high-pressure operation, strict water purity standards, and the system's shorter lifetime when compared to AE systems [39].

The principle of PEM operation is as follows: a polymer membrane with high proton conductivity is used instead of an aqueous electrolyte in this electrolysis cell. Only protons and electrons can be transferred between the electrodes. During the electrolysis process, H_2 is generated in the cathode layer, while O_2 is produced in the anode layer. Fig. 1 represents the technical principle and layout of PEM electrolysis system, the electrode reactions are detailed in Eq. (4) and Eq. (5):

$$\text{Cathode}: 2H^+ + 2e^- \rightarrow H_2 \tag{4}$$

$$\text{Anode}: H_2O \rightarrow 1/2O_2 + 2H^+ + 2e^- \tag{5}$$

For the AE water electrolysis process, hydrogen and oxygen are electrochemically produced from water at the cathode and anode electrodes respectively. In contract to this, water is pumped to the anode in PEM water electrolysis, where it is split into O_2, protons (H^+), and electrons (e^-). The proton conducting membrane transports these protons to the cathode side [40]. The electrons leave the anode by way of the external electricity circuit, which supplies the reaction's driving force in the form of a cell voltage. The protons and electrons recombine to produce hydrogen at the cathode, hence the half-reaction equations for the two technologies differ. PEM electrolysis can produce a purer form of hydrogen (99.99%), whereas the purity of hydrogen produced by AE is 99.5% [41].

The basic technical parameter comparison between PEM and the other two electrolysis systems (AE and SOE) is summarised in Table 1. The PEM is the most adaptable of the three electrolytic systems because it can accommodate rapid ramp up and down as well as intermittent loads, while the AE can only accommodate moderate ramping [40]. The SOE can only operate well under stable conditions [42]. Furthermore, membrane material degradation [43]during the electrolysis process shortens the lifespan of PEM equipment, giving AE the edge in terms of cost-effectiveness and adaptability [44].

Current research directions mainly focus on developing suitable electrode materials and structures such as electrode layers, polymer membranes, and catalysts to reduce infrastructure construction and operating costs; this should make PEM electrolysis technology more cost competitive in the industry sector. Molybdenum disulfide (MoS_2) and related substances have good catalytic activity [45], and according to the findings of Mo et al. [46], the addition of first-row transition metal elements to MoS_2 can enhance the catalytic activity of monolayer MoS_2, particularly Co-^{s}MoS$_2$, which is capable of competing with Pt-based catalysts in industry, and as such is an efficient alternative catalyst material.

2.1.3. Solid oxide electrolysis

In contrast to AE and PEM, superheated steam is used as a feedstock in the SOE technology; a ceramic membrane is utilized as the electrolyte to conduct O^{2-} ions at elevated temperatures. At temperatures ranging from 923 K to 1273 K, SOE cells typically operate at current densities of more than 1.0 A/cm^2 and a single cell voltage of roughly 1.3 V [47]. As a result of the presence of superheated stream, this method consumes significantly less electrical energy than other water electrolysis technologies, allowing for electrical energy savings. The oxygen-ion conducting membrane is required for the electrolysis process to take place. The technological concept and process of SOE system is depicted in Fig. 1, and the electrode reactions are detailed in Eq. (6) and Eq. (7):

$$\text{Cathode}: 2H_2O + 4e^- \rightarrow 2H_2 + 2O^{2-} \tag{6}$$

$$\text{Anode}: 2O^{2-} \rightarrow O_2 + 4e^- \tag{7}$$

The electrolyser lifespan is currently a key barrier to large scale SOE commercialization, because the high operating temperature has a detrimental effect on SOE durability. The yearly degradation rate required for a SOE cell to achieve economically viable status in comparison to low temperature electrolysis has been assessed at 8%, in contrast to the currently observed degradation rate of 17% [48]. The system's efficiency can be irreparably reduced because of heating and cooling which can create tiny cracks on the membrane surface. Thus, a primary objective of on-going research is to identify electrolyser materials that are sufficiently robust when exposed to high temperatures and humidity to ensure long-term performance stability. Hauch et al. [49] discovered that strontium-doped lanthanum manganite may be an excellent anode material due to its stability in thousands of hours of testing; this can be attributed to its porous microstructure. Ni/YSZ has been utilized for over three decades and therefore is still a typical choice for the cathode material. However, as demonstrated by the rapid drop in initial conductivity, Simwonis et al. [50] found that the agglomeration of nickel particles casts doubts on the material's stability. Several additional alternative cathode materials have since been developed, including lanthanide metal-based and titanate-based composites [49].

2.2. Hydrogen production from water thermochemical cycles

Similar to electrolysis, water can be decomposed into oxygen and hydrogen in thermochemical pyrolysis processes. The term "water

thermolysis" refers to the thermal breakdown reaction that occurs in a single step [65]. The reaction system should operate at a reasonably high temperature (greater than 4273 K) [66] because one-step thermolysis requires a considerable amount of heat energy. This high temperature requirement poses a great challenge for large scale industrial utilization. Another challenge is that water thermolysis produces a mixture of hydrogen and oxygen that is easily recombined back into water, which is difficult to sequentially segregate. As a result, one-step water thermolysis is not in commercial or industrial use currently.

To overcome this limitation a lot of research has focused on water thermochemical cycles as a solution to this problem. In these cycles, water molecules first react with supplementary chemicals (such as sulfur – iodine and copper chlorine) to produce intermediary compounds, which then release hydrogen and oxygen. These cycles, which involve several supplementary and intermediary processes, only accept water as a feedstock, and the final products are oxygen and hydrogen, with the supplementary chemicals left in the system for the next cycle [67]. This greatly enhances potential for commercial and industrial application. Thermochemical hydrogen production may be subdivided into three categories: multi-step cycles involving sulfur-iodine (S–I: section 2.2.1) or copper-chlorine (Cu–Cl: section 2.2.2), and two-step cycles using metal oxides (MO_x) [11].

2.2.1. Sulfur-iodine cycle

High temperature heat (above 1200 K) from nuclear reactors was considered a viable energy source for production of transportation fuels such as ammonia (NH_3) and methanol (CH_3OH) after the oil crises of the 1970s; the chemical reactions to break water molecules into oxygen and hydrogen may be optimised to this nuclear heat source [68]. As a result, by the mid-1970s, General Atomics had introduced and developed the sulfur-iodine cycle (S–I) in the United States [69]; this was followed by the European Joint Research Centre (JRC) in Ispra, Italy, the Japan Atomic Energy Agency (JAEA) [70], and further work in Italy [71]. The S–I pilot plant at JAEA in Japan has demonstrated 30 L/h of hydrogen production [70]; France, Canada, China, and Korea started nuclear hydrogen manufacturing initiatives in the 2020s [72–74]. Solar energy can serve as a viable heat source for the S–I cycle [75]. Table 2 depicts the three basic chemical processes (Bunsen reaction, HI decomposition, and sulfuric acid decomposition) in the S–I cycle. When liquid water is added to a system containing gaseous SO_2 and solid I_2 at a temperature in the range between 293 and 393K, an exothermic Bunsen reaction occurs, resulting in the formation of two acids: H_2SO_4 (sulfuric acid) and HI (hydroiodic acid), which are immiscible aqueous concentrated acids. The decomposition of HI is particularly energy expensive and therefore requires a high temperature (Table 2), which has a detrimental impact on the cycle's overall efficiency [76]. One of the key challenges of the S–I cycle is to eliminate water and iodine surpluses, or, to develop separation technologies that require less energy than distillation. In on-going research, the TRL of the S–I cycle is stated as 6 [77], which is lower than the aforementioned water electrolysis hydrogen production technologies (PEM and AE). Fig. 2 depicts the basic concept of the S–I cycle.

A key barrier to the large-scale application of the S–I cycle mainly lies in the optimization of the reaction process, which should consider the following three aspects: ***(1) Improvement of the operating conditions for high-efficiency Bunsen reaction such that more HI and H₂SO₄ can be produced.*** Lee et al. [80] stated that the ideal operating parameters for the Bunsen reaction is 11 mol of excess water and 4 mol of excess iodine at 330 K, whereas the permissible window for the process reaction is between 11 and 13 mol of excess water, and 4–6 mol of excess iodine, at a temperature of 330–350 K. This condition favours obtaining an HI concentration that is over-azeotropic while avoiding iodine solidification and side reactions. Nafees et al. [81] suggested that it is preferable to operate the reactor at roughly 333K, 4 bar(g), with feed concentration ratios of HI/I_2/H_2O of 1/2.8/7.7. ***(2) Separation of HI and H₂SO₄ and subsequent purification following the Bunsen reaction.*** Bai et al. [82] investigated the reverse Bunsen reaction kinetics to determine the reaction mechanism between H_2SO_4 and HI. Their findings revealed that reaction temperature had the greatest impact on the purification of the H_2SO_4 phase, with 99% of contaminants eliminated at temperatures higher than 403 K using N_2 stripping. The iodine concentration was crucial in determining the reactions during the purification of the HI_x phase. By raising temperature, the flow rate of stripping gas, and the concentration of iodine, the purifying effect can be enhanced, and side reactions can be effectively inhibited [82]. ***(3) Improvement of the HI decomposition to H₂ and I₂.*** HI can be decomposed by catalyst to form hydrogen and iodine. Chaubey et al. [83] stated that currently available catalysts include Pt (Platinum)-metal alloys, Pt loaded on supporters, and metal oxide. When it comes to the metals that can be introduced to produce binary catalysts with Pt, Pd (Palladium), Ir (Iridium), Ni (Nickel) and Rh (Rhodium) are frequently mentioned and used. For the supporters of Pt, active carbon, carbon nanotubes, carbon molecular sieve, γ-Al_2O_3 and graphite are all frequently utilized materials for the catalysts; Pt/carbon nanotubes have optimum activity and stability in the temperature range 673–873 K. In addition to catalysis, HI can also be decomposed by electrolysis.

2.2.2. Copper–chlorine cycle

The copper-chlorine (Cu–Cl) cycle was established in 1984 and has the advantage of a lower temperature requirement (about 803 K) than S–I cycle [84]. As a result, its operation and material costs are low, allowing for effective integration with different energy systems, particularly solar and nuclear power plants [11]. The Cu–Cl cycle is a hybrid cycle (using both electrical and thermal energy); it consists of three chemical reactions: electrolysis of aqueous CuCl (cuprous chloride) and HCl (hydrochloric acid) to produce

Table 2
Characteristics of sulfur-iodine water thermochemical cycle hydrogen production technology [78].

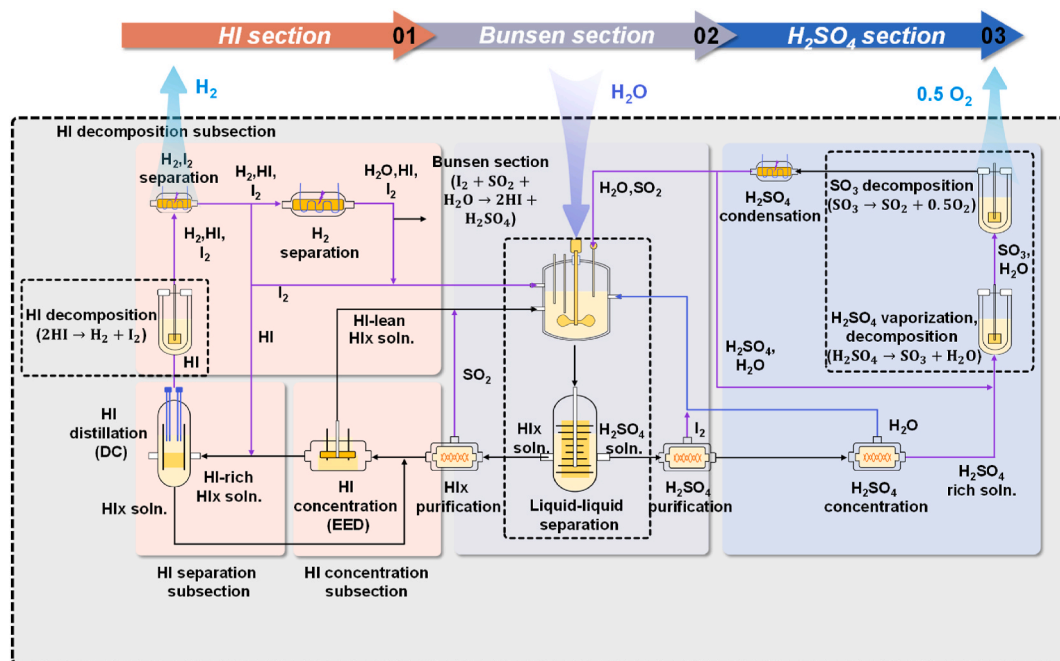| Reaction name	Reactions	Temperature (K)	ΔH (kJ/mol)
Bunsen reaction	$I_2 + SO_2 + 2H_2O \rightarrow H_2SO_4 + 2HI$	293–393	-75 ± 15
HI decomposition	$2HI \rightarrow H_2 + I_2$	1073–1273	186 ± 3
Sulfuric acid decomposition	$H_2SO_4 \rightarrow SO_2 + 1/2O_2 + H_2O$	573–773	12

Fig. 2. Schematic of the sulfur-iodine cycle for sustainable hydrogen production [79] (DC: direct current; EED: electro-electrodialysis; soln.: solution; HI: hydriodic acid; I$_2$: iodine; H$_2$SO$_4$: sulfuric acid; Hix: HI–H$_2$O–I$_2$; SO$_2$: sulfur dioxide; Soln: solution).

hydrogen and CuCl$_2$ (copper dichloride), hydrolysis of CuCl$_2$ with steam to produce Cu$_2$OCl$_2$ (melanothallite), and thermolysis of Cu$_2$OCl$_2$ to produce oxygen [85]. Table 3 outlines the principles of the Cu–Cl cycle.

The Cu–Cl cycle has a low rate of undesirable reactions and produces no greenhouse gases or other pollutants; however, the Cu–Cl cycle technology lacks technological maturity and has a high cost of equipment, which at this TRL precludes large-scale commercial deployment [86]. According to the number of reactions, Cu–Cl cycles can be subdivided into three-step, four-step, or five-step cycles [87]. Different Cu–Cl thermochemical cycles generate hydrogen energy in distinct ways, with distinct heat and mass transfer mechanisms, distinct intermediate products, and ultimately distinct hydrogen yields. Orhan et al. [88] proposed that one disadvantage of the five-step Cu–Cl cycle is the creation of copper chloride (CuCl) and solid copper which increases the number of solid particles transported and handled inside the cycle. Additionally, estimating the mass and heat transfer mechanisms of solid-fluid or solid-solid mixtures becomes increasingly complicated as a result of incomplete reactions, undesirable by-products, and a resulting drop in overall cycle efficiency [88]. This drawback can be overcome through lowering the number of major reactions in the five-step Cu–Cl cycle and so minimising the creation of unwanted solid particles. Additional benefits of reducing steps in the Cu–Cl cycle include improved reaction kinetics, as well as optimised management of gaseous liquids when compared with solid phase components.

However, shortening the Cu–Cl cycle steps may result in additional issues such as increased heat requirement, increased generation of undesired by-products, and decreased output of the desired products. The requirement for a higher-grade source of heat complicates material selection for constructing and developing the Cu–Cl cycle reactors from a practical engineering viewpoint. Using a life cycle assessment model, Ahmet et al. [89] assessed several water thermochemical splitting cycles and determined that the four-step Cu–Cl cycle had less environmental impact than the three- and five-step cycles.

2.2.3. Two-step thermochemical hydrogen production cycles

As observed in Eqs. (8) and (9), a metal oxide serves as an intermediary medium for the breakdown of water during a two-step thermochemical cycle process. Currently available metals are divided into two general categories: volatile metals such as Zn (Zinc)

Table 3
Reaction characteristics of Cu–Cl cycle [11,85].

Reaction name	Reactions	Temperature (K)
Electrolysis of CuCl and HCl	2CuCl(aq) + 2HCl(aq) → H$_2$(g) + 2CuCl$_2$(aq)	298
Hydrolysis of CuCl$_2$	2CuCl$_2$(s) + H$_2$O(g) → Cu$_2$OCl$_2$(s) + 2HCl(g)	298–648
Thermolysis of Cu$_2$OCl$_2$	Cu$_2$Ocl$_2$(s) → 2CuCl(l) + ½ O$_2$(g)	648–803

(aq: aqueous; g: gaseous; s: solid; l: liquid; while aqueous solution appears in liquid form, the liquid subscript represents a molten state of the salt instead of aqueous; drying process: CuCl$_2$(aq) → CuCl$_2$(s) T = 308–353 K.).

Table 4

Recent advances in selected two-step thermochemical cycles.

Redox pairs	Thermo reduction step temperature	Efficiency (LHV)		Characteristics	Reactions	Recent advances
		No heat recovery	With heat recovery (50%)			
SnO_2/ SnO	1780K [96]	36.26% [96]	49.61% [96]	1. Volatile cycle with high reduction temperature requirement. 2. High theoretical energy conversion efficiency. 3. Material loss during reduction process. 4. High SnO hydrolysis rate (98%). 5. Disproportionation reaction at temperatures above 600 °C: SnO → SnO_2 + Sn.	1. SnO_2 (s) → SnO (g) + 0.5 O_2 (g) 2. SnO (s) + H_2O (g)→ SnO_2 (s) + H_2 (g)	As a volatile metal, SnO_2/SnO is often compared with ZnO/Zn in hydrogen production rate, hydrolysis speed, activation energy, reaction orders, and kinetic rate laws [97]. Meanwhile, thermochemical analysis and solar-to-fuel energy conversion efficiency were evaluated by chemistry software and a database [96].
ZnO/Zn	2300K [98]	53.2% [98]	–	1.Volatile cycle with higher reduction temperature requirement than SnO_2/SnO. 2. Fast hydrolysis rate. 3. Insufficient hydrolysis due to ZnO deposition on the surface of Zn. 4. Material loss during reduction process.	1. ZnO (s) → Zn (g) + 0.5 O_2 (g) 2. Zn (s) + H_2O (g)→ ZnO (s) + H_2 (g)	The research directions of ZnO/Zn in recent years mainly focus on: 1. heat transfer mechanism analysis [99]. 2. thermodynamic efficiency evaluation and promotion pathways [100]. 3.Reactor construction [101,102].
	2000K [103] 2300K [104]	14.0% [103] 29% [104]	>30% [103] –			
Fe_3O_4/ FeO	1875K [105]	20.4–25.1% [105]	50.7–62.5% [105]	1. High theoretical energy conversion efficiency. 2. Materials are more likely to sinter and deactivate when the temperature is higher than 2273 K. 3. Non-stoichiometric $Fe_{1-y}O$ is present in the reduction products, which is more active and can hydrolyse quicker. 4. The reduction temperature requirement is lowered by Fe_3O_4 supported on m-ZrO_2 or YSZ.	1. Fe_3O_4 (s) → 3FeO (s) + 0.5 O_2 (g) 2. 3FeO (s) + H_2O (g)→ Fe_3O_4 (s) + H_2 (g)	Recent research mainly focuses on assessing the effect of operation conditions such as temperature, pressure, and steam to feed ratio on the reaction products and conversion rates [106,107].
CeO_2/Ce $O_{2-\delta}$	1873K [108]	0.7–0.8% [108]	–	1. Reduction temperature requirement is lower than ZnO/Zn. 2. Stable circulation. 3. Doping ZrO_2 can increase reduction rate and reduce temperature requirement. 4. Non-stoichiometric Ce $O_{2-\delta}$ can persist steadily in air with high activity	1. CeO_2 → Ce $O_{2-\delta}$ + $\frac{\delta}{2}$ O_2 2. Ce $O_{2-\delta}$ + $\frac{\delta}{2}$ H_2O (g)→ CeO_2 + δ H_2	Since this cycle is still in the laboratory stage, the current research focuses on the study of reaction kinetics and the determination of the optimal reaction conditions [109,110].
	1723–1773K [111] 1800 K [112]	5.25% [111] 20.2% [112]	– 29.5% [112]			
	2300–2600K [113]	23–29% [113]	–			

and Sn (Tin), and non-volatile metals such as Fe (Iron) and Se (Selenium) [90]. The advantages of the two-step thermochemical cycle include the production of oxygen and hydrogen in distinct stages, which eliminates the need to separate them. The ability to use high-temperature heat (1780–2600 K [91]) directly can improve system energy efficiency and decreases the requirement for further power generation procedures. There are still drawbacks (such as the difficulty of selection and implementation of high temperature resistant materials) which place tremendous strain on industrial infrastructure when combined with renewable energy utilization [91].

The thermal reduction step is described in Eq. (8):

$$M\,O_x \rightarrow M\,O_{x-\delta} + \frac{\delta}{2}\,O_2 \qquad (8)$$

The water splitting step is described in Eq. (9):

$$M\,O_{x-\delta} + \delta\,H_2O \rightarrow M\,O_x + \delta\,H_2 \qquad (9)$$

Where M are specific metals, such as Zn, Sn, Ce, or Fe. Table 4 depicts recent advances in selected two-step thermochemical cycles. Current research activities on two-step thermochemical cycles can be separated into three distinct phases. The initial phase is identifying, testing, and developing appropriate metal oxide materials (MOx in Eqs. (8) and (9)). The second phase involves the examination of two-step cycles at a laboratory scale. The third phase involves the implementation of pilot testing and optimization of the system. At temperatures between 1573 and 1773 K, Antoine et al. [92] observed that doped-ceria and spinel ferrite were the most suitable materials which exhibited strong hydrolysis abilities. Apart from these two materials, no material could produce hydrogen efficiently below 1373 K in literature on the thermochemical hydrogen production cycles. Non-volatile non-stoichiometric oxides (δ in $M\,O_{x-\delta}$ is not an integer but a decimal number) such as zirconium oxide have provided a new route for the development of thermochemical materials for renewable energy production due to their superior thermo-kinetic characteristics for hydrogen production, good structural stability, and moderate reduction temperature [93]. Heat recovery is crucial to improve the energy conversion efficiency. The inclusion of an oxygen exchange membrane provides the potential for inert gas recovery, and alterations of the catalyst structure should also be taken into account [94]. Solar thermochemical hydrogen production at 1673 K has been proven at a pilot scale, according to Abanades et al. [95]; this establishes a significant benchmark for future development.

2.3. Hydrogen production from biomass

Biomass can be derived from a variety of sources, including grasses, wood, crop residues, agricultural products, animal and plant wastes, food scraps, municipal wastes and algae, and is viewed as a viable substitute for fossil fuels [114]. Direct hydrogen production from biomass can be achieved in two ways according to the mechanism of gas generation: thermochemical processes (including gasification, pyrolysis, and liquefaction techniques [66]) or biological processes (including dark/photo fermentation and

Table 5

Characteristic comparison of steam gasification and supercritical water gasification technologies.

Technology	Steam gasification	Supercritical water gasification
Reaction process	$C + H_2O \rightarrow H_2 + CO$ $CO + H_2O \rightarrow H_2 + CO_2$ $CH_4 + H_2O \rightarrow 3H_2 + CO$ $C_aH_b + aH_2O \rightarrow (a+b)H_2 + aCO$ [118]	$CH_nO_m + (1\text{-}m)H_2O \rightarrow (n/2+1\text{-}m)H_2 + CO$ $CO + H_2O \rightarrow H_2 + CO_2$ $CO + 3H_2 \rightarrow CH_4 + H_2O$ $CO_2 + 4H_2 \rightarrow CH_4 + 2H_2O$ [119]
Product gas heating value, MJ/Nm^{-3}	High 15–20 [120]	High 15–20 [120]
Average H_2 production (wt%, g H_2/100 g	Without catalyst: 4g With catalyst: 7g [115]	Without catalyst: 3g With catalyst: 5g [115]
Typical biomass	Lignocellulose, algae, wood saw dust, waste wood, paper, coffee husk, almond shell [117]	Sewage sludge, aqueous sludge, contaminated wastewater, coal wastewater, chicken manure [117]
Reactor	Fluidized bed; upper/lower ventilation gasifier [115]	Continuous reactor; batch reactor [115]
Reactor temperature (K)	973-1473 [117]	663-973 [117]
Catalyst	Dolomite, Ni based catalyst, alkaline metal, alumina, K_2CO_3, Na_2CO_3, ZnCl [121]	K_2CO_3, Na_2CO_3, KOH, NaOH, ZrO_2, Ni/ZrO_2 [121]
Influential operating parameters	Biomass characteristics, temperature, steam-to-biomass ratio [122]	Temperature, operating pressure, reactant concentration, reaction time [122]
System energy efficiency (LHV)	40–50% [122]	40–50% [122]
Technology readiness level	8 [123]	8 [123]
Advantages	Potential for large-scale industrial production because of minimal ash production and high gasification rate.	High gasification rate without the generation of tar, coke, or secondary pollution.
Disadvantages	Difficult to separate and purify the gas products.	Strict operating conditions and difficult alkaline catalysts recycling process.
Challenges	Reduce tar concentration; develop appropriate catalyst; improve technology readiness level and reduce technology construction and operating costs.	Improve technology readiness level and reduce technology construction and operating costs.

(LHV: low heating value; wt: weight).

bio-photolysis).

2.3.1. Biomass gasification

Biomass gasification is partial oxidation of biomass compounds in presence of air, oxygen or steam to produce gases mainly including of CO, CO_2, CH_4 and H_2. Methane and other hydrocarbons such as tars and char are also produced. In comparison to other waste processing techniques such as landfilling and incineration, biomass gasification has a higher potential for application because it can accept a wide range of inputs, including for diverse feedstocks such as wood and algae, and produce multiple useful products, including hydrogen and carbon monoxide [115].

Drying the feedstock is the first step in the complex process of biomass gasification, which also involves pyrolysis, partial combustion of intermediates, and gasification of the final products. The process is carried out inside a gasifier with the presence of gasifying media which can be air, steam (H_2O), oxygen (O_2), or carbon dioxide (CO_2) [116]; the gasifying media has a significant impact on the product gas calorific value. The heating value can be in the range 4–7 MJ Nm^{-3} for the product gas from air gasification (due to the presence of nitrogen in air), whereas it can rise up to the range of 12–28 MJ Nm^{-3} when oxygen is used as gasifying media (excluding nitrogen in the producer gas) [15].

By lowering the carbon-to-hydrogen (C/H) mass ratio, biomass gasification enhances the product's calorific content due to an increased H_2 fraction. The gasifying media is essential for turning heavy hydrocarbons and solid char into low-molecular-weight gases like hydrogen and carbon monoxide. The gasifying media, feedstock material, reactor design, reactor temperature and pressure, and catalyst type all play significant roles in the quality of product gas [117]. The two commonly used thermochemical biomass-to-hydrogen technologies are steam gasification and supercritical water gasification with comparisons detailed in Table 5.

For both steam gasification and supercritical water gasification, the introduction of a catalyst can reduce the temperature requirement of the reaction, and promote condensable fraction reforming and tar cracking. Tar is a substantial issue in the biomass gasification process as it can clog equipment (heat exchangers), raise maintenance costs, and complicate overall operation [124,125]). To enhance hydrogen production and carbon conversion efficiency, more recent research has focused on the design and selection of appropriate catalysts. According to Okolie et al. [126], typical alkaline metal catalysts can accelerate the steam gasification and supercritical water gasification process effectively, however, there are limitations such as the difficulty of catalyst recovery, significant loading on the catalyst, and blockages. Chan et al. [127] stated that noble metals, notably Rh (Rhodium) and Ru (Ruthenium), exhibit good catalytic activity in both pathways but cannot be employed widely due to cost constraints. Gai et al. [128] proposed that Ni (nickel)-based catalysts have been commonly utilized as effective catalysts and that it is preferable to employ them in conjunction with other metals. Because of the high solubility in water at high temperatures, the frequently employed Al (Aluminium)-based catalysts for steam gasification are not optimal for supercritical water gasification. According to Gholkar et al. [129], not only do metal oxides possess catalytic activity, but they may also be effective supporters for external metal catalysts: a metal oxide supporter can increase
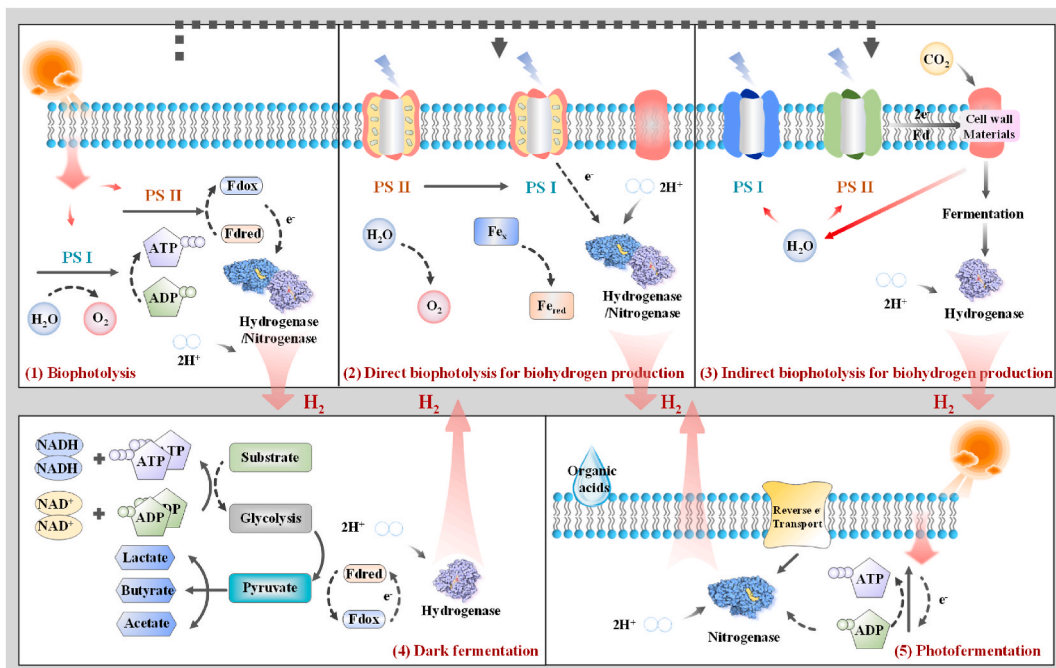

Fig. 3. Principle of biological hydrogen production technologies. (1) biophotolysis, (2) direct biophotolysis for biohydrogen production, (3) indirect biophotolysis for biohydrogen production, (4) dark fermentation, (5) photofermentation [144] (ATP: adenosine triphosphate; ADP: adenosine diphosphate; Fdred: ferredoxin; Fdox: flavodoxin; PSI: photosystem I; PSII: photosystem II; NADH: nicotinamide adenine dinucleotide hydrogen).

Table 6
Technological characteristics of different biohydrogen production process.

	Direct biophotolysis [145,146]	Indirect biophotolysis [147,148]	Photo fermentation [149,150]	Dark fermentation [151–153]
Substrate	H_2O	H_2O, CO_2	- Simple sugars - Organic wastes	- Simple sugars - Organic wastes
Microorganism	Green algae, cyanobacteria	Cyanobacteria	Photoheterotrophic bacteria (*Rhodobacter, Rhodobium, Rhodopseudomonas,* and *Rhodospirillum* strains)	Obligate or facultative anaerobe fermentative bacteria (*Alcaligenes, Bacillus, Clostridia, Citrobacter, Enterobacter, Escherichia coli*)
Reaction	$2H_2O + light \rightarrow 2H_2+O_2$	1: $6CO_2 + 6H_2O \rightarrow C_6H_{12}O_6 + 6O_2$ 2: $C_6H_{12}O_6 + 6H_2O \rightarrow 12H_2 + 6CO_2$	$CH_3COOH+2H_2O + light \rightarrow 4H_2+2CO_2$	*Acetic Acid Pathway:* $C_6H_{12}O_6 + 2H_2O \rightarrow 4H_2+2CO_2+2CH_3COOH$ *Butyric Acid Pathway*: $C_6H_{12}O_6 + 2H_2O \rightarrow C_4H_8O_2 + 2CO_2 + 4H_2$
Light/energy requirement	Yes	Yes	Yes	No
By-products	O_2	CO_2, O_2, metabolites	Volatile fatty acids (VFAs such as proprionic acid, butyric acid, acetic acid), Ethanol	Volatile fatty acids (VFAs such as proprionic acid, acetic acid), Methanol, Butanol, Acetone
Parameters affecting H_2 yield	- Light intensity - Medium composition - Microorganism type - Photobioreactor design	- Light intensity - Medium composition - Microorganism type - Photobioreactor design	- Medium composition - Microorganism type - Light intensity - Type of substrate - Photo-fermenter design	- Type of substrate - Medium composition - Microorganism type - Fermenter design
Gases produced	- H_2, O_2	- H_2, O_2, CO_2	- H_2, CO_2	- H_2, CH_4, CO_2, CO, H_2S
Advantages	- Simple substrate: H_2O - CO_2 consumption - Simple condition for cultivation	- Separate the requirements for O_2 and H_2 production. - Capable of fixing N_2 from air (to generate nitrogenase) - Metabolite by-product converted to H_2	- Process broad range of substrates - Bioremediation - Process effluent from dark fermentation - Photosynthetic bacteria can use a broad spectrum of light	- Process broad range of substrates - Bioremediation - Process independent of light - The created by-products bring value to the process - O_2 restriction is of no concern
Opportunities	- Genetic and metabolic engineering - Optimization of culture conditions, light usage efficiencies, and reactor design	- Avoid H_2 consumption by the hydrogenase enzyme. - Investment and operation cost reduction	- Optimization of substrate usage, process, and reactor design - Genetic engineering - Cell immobilization	- Genetic engineering - Optimization of substrate utilization, process, and reactor design
Considerations for commercialization	- Demand high light intensity - Demand bioreactors with huge surface areas - Reduction of O_2-sensitivity - Formation of explosive O_2–H_2 mixture - Low photochemical efficiency	- Demand high light intensity - Demand bioreactors with huge surface areas - Elimination of uptake hydrogenase to avoid H_2 decomposition	- Substrate pre-treatment - Insufficient light conversion efficiencies - Inhibition of hydrogenase by O_2	- Substrate pre-treatment - Insufficient substrate conversion efficiency - Low H_2 purity in gaseous product mixture - Relatively lower H_2 yield

the stability of Ni-based catalysts.

To enhance system operation efficiency and hydrogen production efficiency, much research on biomass gasification has focused on optimizing operating parameters, such as (1) selection of the type, quality and moisture content of the biomass feedstock; (2) developing appropriate density and particle size of the feedstock; (3) investigating steam-to-biomass ratios; (4) finding the applicable air equivalence ratio (the proportion of actual air supplied as compared to the stoichiometric air required for the operation). Schuster et al. [15] claimed that more gaseous products can be produced during gasification by appropriately increasing the ratio of cellulose and hemicellulose to lignin in biomass. Despite the fact that reducing particle size enhances syngas efficiency and decreases tar yields, the particle size should not be decreased below the minimum required level since particle size reduction requires a substantial amount of extra energy input. According to Nader et al. [130], a rise in temperature increases the heating rate of the feedstock particles by producing a wider temperature difference, thus promoting an increase in the reaction rate. Jun et al. [131] found that an increase in air equivalence ratio decreased H_2 and CO yield whilst increasing CO_2 concentration, consequently reducing the calorific value of the generated gas.

2.3.2. Biological conversion

Biological hydrogen production includes two typical processes: bio-photolysis and fermentative biohydrogen generation [132]. Certain microbes are capable of splitting water and producing H_2 under light-driven circumstances during the bio-photolysis process; this process can further be classified as direct or indirect bio-photolysis with green algae and cyanobacteria as representative microorganisms. Fermentation (including dark and photo fermentation) is a biological reaction in which microbes convert organic compounds (such as starch and cellulose) to alcohols, acetone, H_2, and CO_2 under aerobic or anaerobic conditions. The TRL for both direct and indirect biophotolysis is 4 [133], whereas for photofermentation is 4 [134], and dark fermentation is 7 [135]. Fig. 3 depicts the principle of biological hydrogen production technologies, and Table 6 presents a comparison of the different ways for biohydrogen production.

Bio-photolysis is characterised by low H_2 yields (the photo-hydrogen-energy conversion efficiency is less than 10%) [136], due to inefficient light conversion and oxygen sensitivity of the process. Utilising O_2-binding proteins allows for the control of O_2 production during the photosynthesis process. Adding an inert gas to the reactor headspace can also assist in minimising O_2 concentrations, however, this process entails a significant operational expenditure. One effective strategy for enhancing H_2 production is through genetic and metabolic engineering of cyanobacteria and green algae to increase the light conversion efficiency [137,138]. Additionally, direct bio-photolysis might cause safety issues since the mixture of O_2 and H_2 could be explosive. Furthermore, this light-driven process produces hydrogen gas only when microalgae are exposed to light. While sunlight is a reasonably affordable energy source, the system might still need artificial illumination to further increase hydrogen production efficiency, thereby increasing the cost of bioreactors and increasing energy expenses [139]. Other parameters affecting biohydrogen output include microalgae light-capturing and CO_2 fixation efficiency [140]. Many techniques for optimizing H_2 generation via bio-photolysis have been investigated including; bioreactor construction, bioprospecting [141], genetic and metabolic engineering of microalgae [142], as well as optimizing culture and process parameters [143].

Further research to improve the maturity of biohydrogen production should focus on selecting appropriate microorganisms, pretreatment of substrates, process and reactor parameter optimization, and H_2 extraction from product gases. Lee et al. [154] suggested that dark fermentation is kinetically faster than photo-fermentation or bio-photolysis, however, the liquid by-products from dark fermentation such as lactic acid ($C_3H_6O_3$), butyric acid ($C_4H_8O_2$), acetic acid (CH_3COOH), butanol ($C_4H_{10}O$), methanol (CH_3OH), or acetone (C_3H_6O), limit the maximum efficiency of H_2 generation. It was thus recommended to select and domesticate mixed cultures to reduce by-product generation and improve hydrogen formation rates. Singh and Wahid [155] claimed to use immobilized whole cell techniques in photo and dark fermentation to improve the efficiency of hydrogen production.

3. Cost and life cycle environmental impacts comparison

3.1. Cost analysis

3.1.1. Cost of hydrogen from electrolysis

The costs of water electrolysis-based hydrogen production technologies can be categorized under capital expenditures (CAPEX, including the cost of electrolyser, liquid compressor, gas compressor, storage tank, electricial connection, heater, installation and indirect cost [156]) and operating expenditures (OPEX, including the cost of electricity, maintenance, labour, water and fixed operation & management [157]). The levelized cost of hydrogen (LCOH) is a parameter that can be utilized to compare the costs of different hydrogen production techniques. LCOH is defined as the ratio of the overall costs (including CAPEX and OPEX) throughout the full project duration to the total quantity of energy carrier produced at the same time [158]. The LCOH equation can be expressed as per Eq. (10), where t denotes the year number during the lifetime of the hydrogen production plant, C_t represents cost at "t", Q_t is the amount of hydrogen produed at "t", I_0 refers to initial investment cost, and r represents discount rate.

$$\text{LCOH} = \frac{I_0 + \sum_{t=0}^{n} \frac{C_t}{(1+r)^t}}{\sum_{t=o}^{n} \frac{Q_t}{(1+r)^t}} \tag{10}$$

The cost of reliable zero-carbon electricity (such as from wind or solar energy) equates to roughly 50%–55% of the LCOH on

average [51]. The capital cost of the electrolyser accounts for 15%–20% of the LCOH [159]. Financing and fixed operating costs (such as plant upkeep and maintenance) represent approximately 18%–24% of the LCOH [160]). The magnitude and variety of these costs have a significant impact on the LCOH when producing green hydrogen. In the existing literature on techno-economic modeling analysis of hydrogen production through water electrolysis, the LCOH ranges between 2.34 and 6.55 €$_{2021}$/kg [156,161,162]for AE technology and 3.77–9.50 €$_{2021}$/kg [163–165]for PEM technology. However, most of these ranges are based on theoretical mathematical modelling and do not account for complex factors encountered in practical engineering applications (such as taxes, the fluctuation of renewable electricity price, and regional costs of renewable energy acquisition). Therefore, the actual LCOH of hydrogen production in industrial applications is expected to be relatively higher than that of the theoretical estimates. Zhiyuan et al. [157] assessed LCOH values for different electrolysis technologies in different regions based on data from the IEA (International Energy Agency) and IRENA (International Renewable Energy Agency). They found that for a typical PEM electrolyser facility of 10 MW capacity in the EU, the average LCOH would be 11.06 €$_{2021}$/kg and 11.61 €$_{2021}$/kg for wind and solar scenarios respectively (a higher capacity factor is largely responsible for the relatively lower LCOH for the wind scenario than that of solar utility in the EU). Minutillo et al. [166]assessed the on-site hydrogen refueling stations using grid connected PV plants and electrolysis units in Italy. Their results indicated that LCOH from AE technology ranges from 9.29 to 12.48 €$_{2021}$/kg. However, existing literature widely acknowledges that the cost of producing renewable electricity continues and will continue to decline with technology advancement and economies of scale [86,167,168], resulting in the LCOH to be declined to the range of 4.15–5.84 €$_{2030}$/kg in 2030 [157].

For the three water electrolysis-based hydrogen production technologies, it is also anticipated that electrolyser CAPEX will decrease over time, lowering the cost of green hydrogen across all regions (especially for PEM and SOE) [169]. Glenk and Reichelstein [170] presented historical cost estimates up to 2016 and projections through to 2030. They projected yearly CAPEX savings of 3% for AE and 4.8% for PEM but did not predict the trend for SOE. Schmidt et al. [26] estimated the CAPEX of alkaline electrolysis cell (AEC), polymer electrolyte membrane electrolysis cell (PEMEC), and SOEC at 870, 1263, and 2854 €/kW in 2020, decreasing to 611, 978, and 1902 €/kW in 2030 respectively; this is higher than the estimate from Glenk and Reichelstein [170]. PIK (2021), on the other hand, conducted an updated CAPEX assessment of the cost and efficiency trend for AEC, PEMEC, and SOEC and projected the quantitative results to 2050 [60], as shown in Fig. 4.

3.1.2. Cost of hydrogen from thermochemical cycles

There is on-going investigation into the direct use of nuclear heat for water molecule splitting using thermochemical cycles. The
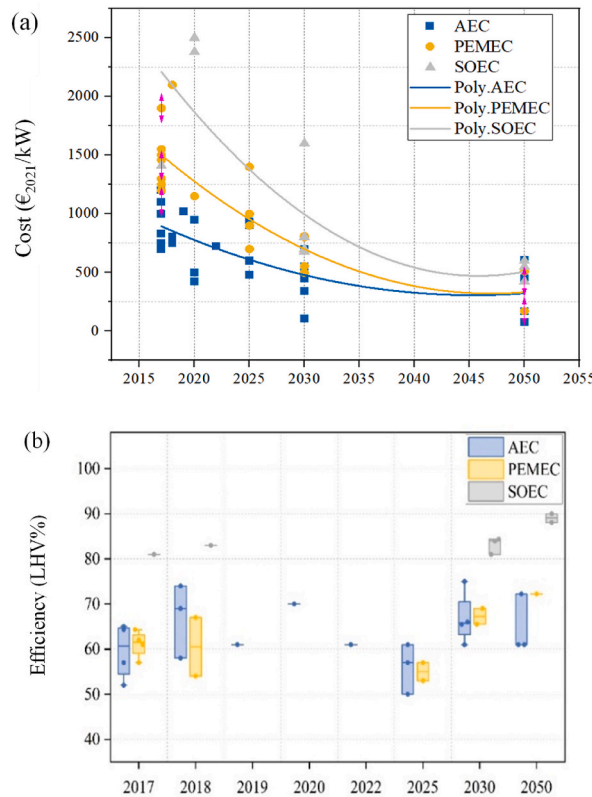

Fig. 4. Cost reduction trend and efficiency of AEC, PEMEC, and SOEC to 2050. (a): cost reduction trend; (b) efficiency development (Data source: PIK) [60]. (AEC: alkaline electrolysis cell; PEMEC: polymer electrolyte membrane electrolysis cell; SOEC: solid oxide electrolysis cell; poly: polynomial fitting function).

Cu–Cl and S–I cycles are currently the most promising low-temperature and high-temperature cycles respectively [171]. The LCOH of S–I and Cu–Cl cycles is suggested to lie between 6.72 and 10.15 €$_{2021}$/kg H$_2$ [172–174] and 5.54–7.58 €$_{2021}$/kg H$_2$ [175,176], respectively, with averages of 8.44 €$_{2021}$/kg H$_2$ and 6.56 €$_{2021}$/kg H$_2$. Due to the lack of large-scale industrial application of water thermochemical cycles, the LCOH values from literature are mostly based on software simulations and assume an ideal environment; such assessments must be seen as relatively indicative as they may not include for inefficiencies across the system such as heat loss and pressure drop in the transfer process [177]).

Plant capacity, as well as other parameters such as H$_2$ production capacity, plant efficiency, and electricity cost, have a considerable impact on the cost of hydrogen, with published figures shifting significantly based on these input parameters even for the same type of energy source (such as nuclear or solar energy) and technology [178]. Cost data for the thermochemical cycle is limited, with few studies disclosing the capital cost data needed to calculate the LCOH. As a result, the LCOH estimations are subject to large and unquantifiable uncertainty. Currently the thermochemical cycles have only been deployed in pilot-scale testing by the Atomic Energy Agency of Japan [179] and further research and development by the Idaho National Laboratory [180]. Large-scale hydrogen production plants would be necessary to match the heat provided by nuclear facilities and to reduce the cost of hydrogen production.

3.1.3. Cost of biomass-based hydrogen

Existing biomass gasification and biological conversion hydrogen production technologies do not have large-scale commercial applications, and therefore rely on system model simulations to calculate cost data. It is difficult to obtain normative parameters for techniques that are still in small-scale production. The inventory data that are utilized for the assessment either require additional self-defined parameters or are distinct from one another; this results in very disparate values for cost evaluation of biomass-based hydrogen production in the literature. Table 7 depicts estimations of hydrogen production cost from biomass gasification and biological conversion. Pallozzi et al. [181] investigated a 1 MWth input biomass gasification hydrogen production plant at a temperature of 573 K with a steam to biomass ratio of 2.0; the LCOH was estimated to be 8.3 €$_{2016}$/kg (10.85 €$_{2021}$/kg; Chemical Engineering Plant Cost Index (CEPCI) is used to update the LCOH value; CEPCI$_{2016}$ = 541.7; CEPCI$_{2021}$ = 708.0 [64]). Hamedani et al. [182] conducted a techno-economic analysis of a small-scale (100 kWth) hydrogen production system using biomass gasification and estimated the LCOH to be 12.75 €$_{2016}$/kg (16.66 €$_{2021}$/kg).

The LCOH of dark fermentation in literature is estimated to be between 14.83 and 39.25 €$_{2021}$/kg [135,183–186], while the LCOH range of biomass gasification is expected to be 10.85–18.43 €$_{2021}$/kg [181,182,187]. The technological development of biomass-based hydrogen production remains highly uncertain until 2030, and therefore, its cost changes cannot be predicted with the same level of confidence as that for water electrolysis.

3.2. Life cycle environmental impact assessment

The utilization of Life Cycle Assessment (LCA) as an environmental impact assessment technique for products and services is well-established [188]. In accordance with ISO standards 14040 and 14044 [189,190], this methodology is structured into four distinct stages. Firstly, the "Goal and Scope Definition" phase is employed to establish the objective of the assessment and define the system boundaries. Secondly, the "Life Cycle Inventory Analysis" stage entails assuming and calculating all pertinent input and output

Table 7
Estimated costs of hydrogen production from biomass gasification and biological conversion.

Feedstock	H$_2$ production method	Plant details	Capital expenditure	Operating expenditure	Revenue from H$_2$	LCOH	Updated LCOH	Ref.
Food waste	Dark fermentation	Plant capacity - 2 ton/day; Lifetime - 10 years	931,020 €/a	299,746 €/a	639,920 €/a	14.91 €$_{2016}$/kg	19.49 €$_{2021}$/kg	[183]
Molasses	Dark fermentation	Plant capacity- 50 m^3; Lifetime - 10 years	478,200 €/a	262,170 €/a	331,121 €/a	30.03 €$_{2016}$/kg	39.25 €$_{2021}$/kg	[184]
Food waste	Dark fermentation	plant capacity- 3 ton/day; Lifetime - 15 years	583,092 €/a	88,298.1 €/a	146,473.6 €/a	11.35 €$_{2016}$/kg	14.83 €$_{2021}$/kg	[185]
Wastewater	Dark fermentation	Plant capacity- 10 m^3; Lifetime - 10 years	1,615,000 €/a	1,227,000 €/a	328,000 €/a	30.03 €$_{2012}$/kg	36.37 €$_{2021}$/kg	[135]
Agricultural waste	Dark fermentation	Plant capacity -10m^3; Lifetime - 10 years	2,097,000 €/a	1,238,000 €/a	328,000 €/a	30.03 €$_{2016}$/kg	39.25 €$_{2021}$/kg	[135]
Food waste	Dark fermentation	Plant capacity- 10 ton/day; Lifetime - 10 years	707,850 €/a	366,700 €/a	574,800 €/a	25.47 €$_{2016}$/kg	33.29 €$_{2021}$/kg	[186]
Lignocellulose biomass	Gasification	Biomass feeding rate - 20 kg/h; Lifetime −20 years	76,910 €/a	46,790 €/a	3700 €/a	12.75 €$_{2016}$/kg	16.66 €$_{2021}$/kg	[182]
Almond shell	Gasification	Biomass feeding rate - 20 kg/h; steam feeding rate – 20 kg/h	60,700 €/a	39,900 €/a	3625 €/a	10.37 €$_{2016}$/kg	13.55 €$_{2021}$/kg	[182]
Hazelnut shell	Gasification	Constant flow rate – 200 kg/h (1000 kW$_{th}$) with a moisture content of 10%	1625.76 €/a	847.27 €/a	276.51 €/a	8.3 €$_{2016}$/kg	10.85 €$_{2021}$/kg	[181]
Nutshell	Gasification	Steam to biomass ratio – 1kg$_{steam}$/kg$_{biomass}$	603,420 €/a	420,904 €/a	372,482 €/a	15.7 €$_{2018}$/kg	18.43 €$_{2021}$/kg	[187]

(CEPCI: Chemical Engineering Plant Cost Index; CEPCI$_{2012}$ = 584.6; CEPCI$_{2016}$ = 541.7; CEPCI$_{2018}$ = 603.1; CEPCI$_{2021}$ = 708.0 [64]).

parameters. Thirdly, the "Life Cycle Impact Assessment" stage is implemented to quantify the environmental consequences associated with the evaluated process chain. Lastly, the "Life Cycle Interpretation" phase is undertaken to deliberate upon the findings. A range of studies examing hydrogen production have been conducted using LCA methods. Delpierre et al. [191] used LCA methods to compare the environmental impacts of large-scale AE and PEM systems for CO_2-free hydrogen production in the Netherlands. Their results show that both systems have similar environmental impacts, with the electrolyser contributing to only 10% of the total impact. The origin of
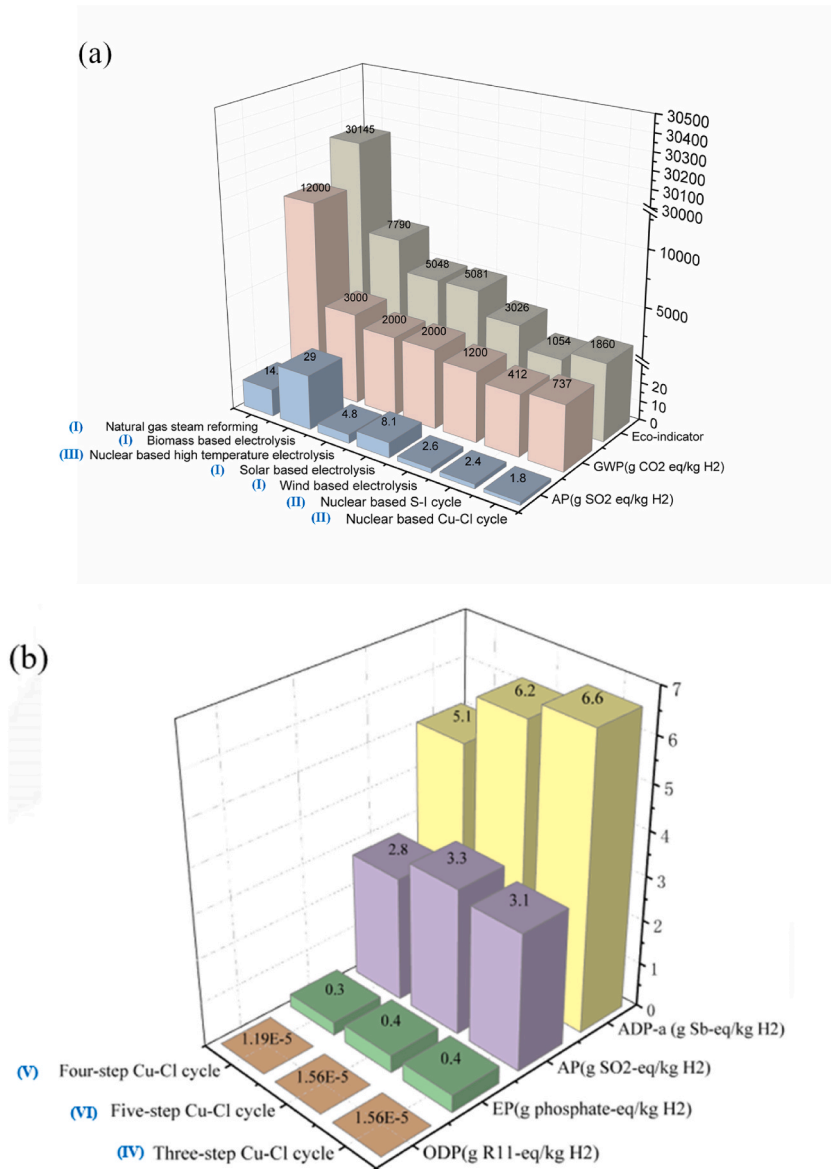
Fig. 5. LCA analysis results of different sustainable hydrogen production technologies. (a) GWP, AP and Eco-indicator value; (b) ODP, EP, AP and ADP-a value [197] (AP: acidification potential; ADP-a: abiotic resource depletion potential; EP: eutrophication potential; GWP: global warming potential; ODP: ozone depletion potential). System assumptions: (I) National Renewable Energy Laboratory provide GWP information for hydrogen produced by traditional natural gas steam reforming, wind and solar based electrolysis [196]. (II) Plant capacity 3000 kg H_2/day; overall inputs for 1 h of operation of hydrogen production plant (thermal energy 18.57 GJ; water 1125 kg); overall output for 1 h of operation of hydrogen production plant (hydrogen 1125 kg), heat exchanger efficiency (HHV) = 50% [198]. (III) Nuclear based high temperature electrolysis plant requirement: electrical energy 200 MJ/kg H_2, thermal energy 35 MJ/kg H_2. Hydrogen production rate 7700 kg/h; plant capacity 600 MW [199]. (IV) Three-step Cu–Cl cycle hydrogen plant overall inputs: thermal energy 182.74 MJ/kg H_2; electrical energy 67.15 MJ/kg H_2; water 9 kg/kg H_2. Plant outputs: oxygen 8 kg/kg H_2; hydrogen 1 kg [197]. (V) Four-step Cu–Cl cycle hydrogen plant overall inputs: thermal energy 161.05 MJ/kg H_2; electrical energy 67.15 MJ/kg H_2; water 9 kg/kg H_2. Plant outputs: oxygen 8 kg/kg H_2; hydrogen 1 kg [197]. (VI) Five-step Cu–Cl cycle hydrogen plant overall inputs: thermal energy 195.7 MJ/kg H_2; electrical energy 50.3 MJ/kg H_2; water 9 kg/kg H_2. Plant outputs: oxygen 8 kg/kg H_2; hydrogen 1 kg. Plant capacity for three Cu–Cl cycles: 125,000 kg H_2/day. Plant lifetime: 60 years [197].

electricity, even when derived from renewable sources, is the main contributor to environmental impact, emphasizing the need for clean energy sources in hydrogen production. Zhang et al. [192] conducted a comprehensive life cycle assessment (LCA) for three solar-based hydrogen production methods. Their results indicate that the thermochemical water splitting method using the S–I cycle coupled with solar photothermal technology exhibits low global warming potential (GWP) (1.02 kg CO_2-eq/kg H_2) and acidification potential (6.56E-3 kg SO_2-eq/kg H_2), demonstrating significant environmental advantages in the overall ecosystem impact. Bhandari et al. [193] conducted a LCA of hydrogen production via electrolysis and found 96% of GWP is associated with the set up of the turbine and H_2 compression/storage in wind electrolysis. In the context of hydrogen production technologies of this paper, the system boundary is limited to the cradle-to-gate perspective, whereby the "gate" refers to the end of the hydrogen production unit [194].

Natural gas steam reforming technology (for grey hydrogen) was employed as a control in previous studies for comparison to make the results of LCA analyses of different sustainable hydrogen production technologies more relative [195]. Fig. 5(a) depicts the GWP, acidification potential (AP), and eco-indicator (equivalent to 10 times the acidification potential value plus 2.5 times the GWP value) of seven hydrogen production techniques. The nuclear based S–I cycle showed the lowest GWP (412 g CO_2-eq/kg H_2; 3.4 g CO_2/MJ), whereas natural gas steam reforming had the highest (12000 g CO_2-eq/kg H_2; 100 g CO_2/MJ). In terms of AP, nuclear based Cu–Cl cycle displayed the lowest value (1.8 g SO_2-eq/kg H_2; 0.015 g SO_2/MJ) while biomass-based electrolysis showed the highest value (29 g SO_2-eq/kg H_2; 0.242 g SO_2/MJ) [196]. An eco-indicator was used to represent or assess the entire environmental impact by Ozbilen et al. [197]. When compared to steam reforming, the results revealed that producing hydrogen using renewable energy-based electrolysis and a nuclear-based thermochemical cycle had a substantially lower environmental impact.

It should be emphasised that the emissions from natural gas steam reforming or biomass-based hydrogen production are fundamentally different from those from water electrolysis technologies powered by nuclear, wind, or solar energy. The plant operation, which occurs continuously, is the main contributor to the emissions from natural gas steam reforming and biomass-based hydrogen production. Conversely for electrolysis-based technologies, mining, manufacturing, and construction phases make up a large portion of the emissions, while plant operation itself makes up a minor portion; these initial processes prior to hydrogen production will lead to an initial significant amount of emissions, followed by relatively lower emissions over the period of plant operation (20 or so years). In order to decrease the environmental impact, acid gas neutralisation and carbon dioxide sequestration technologies may be effective [198].

For the water thermochemical cycles, Ozbilen et al. [197] published a comparison of life cycle assessments for three-, four- and five-step Cu–Cl cycle designs. Fig. 5(b) depicts the results of their analysis in terms of abiotic resource depletion potential (ADP-a), AP, ozone depletion potential (ODP), and eutrophication potential (EP) of hydrogen production from three-, four-, and five-step Cu–Cl cycles based on nuclear energy. Because of the lower thermal energy required, the four-step Cu–Cl cycle has the lowest AP value (2.8 g SO_2-eq/kg H_2; 0.023 g SO_2/MJ), whereas the three-step Cu–Cl cycle has the greatest AP value (3.3 g SO_2-eq/kg H_2; 0.028 g SO_2/MJ). The four-step Cu–Cl cycle also has the lowest ADP-a (5.1 g Sb-eq/kg H_2; 0.043 g Sb/MJ). The EP value indicates the effects of high macronutrient concentrations in the environment, and the values of three-, four- and five-step Cu–Cl cycles are similar (approximately 0.4 g Phosphate-eq/kg H_2; 0.003 g Phosphate/MJ). ODP implies depletion of the stratospheric ozone layer because of emissions and increased ultraviolet radiation. Their results revealed that four-step Cu–Cl cycle has the lowest ODP values, while three-step and five-step Cu–Cl cycles are almost identical.

4. Conclusions

This paper compared the research status, technology readiness level, characteristics, and large-scale deployment barriers of several hydrogen production techniques. Polymer electrolyte membrane electrolysers have the advantages of high energy efficiency (58%–65%), high purity of generated hydrogen (99.999%), relatively short response time to rapid power changes (milliseconds), and the ability to combine variable renewable electricity producers. Optimistic scenarios suggest that the levelized cost of green hydrogen from polymer electrolyte membrane water electrolysis will be in the range of 4.15–6 €/kg in 2030, and thus is suitable for large-scale industrial application in the near term. The sulfur-iodine cycle and copper-chlorine cycle have the greatest potential for large-scale application among the thermochemical cycles. These two technologies are suitable for combination with nuclear energy to generate sustainable hydrogen at expected relatively low prices typically in the range 5.5–10.2 €$_{2021}$/kg H_2. However, it is difficult to predict future prices due to the lack of present commercial applications of the technology. Biomass gasification processes (steam gasification and supercritical water gasification) offer significant potential in geographic regions with widespread availability of woody crops (such as in Canada and Scandinavian countries) for the production of large quantities of syngas. As a relatively mature technology (TRL 8), large-scale biomass gasification industrialization can be achieved in the near term should this technology effectively solve the issue of tar formation and product gas separation. With the issue of cost unpredictability (the levelized cost of hydrogen via dark fermentation is suggested to be in the range 14.83–39.25 €$_{2021}$/kg) and low system efficiency (less than 10% of direct biophotolysis), biological conversion technologies still need considerable development to be competitive with PEM water electrolysis technology.

CRediT authorship contribution statement

administration, Supervision, Validation, Writing – review & editing.

Declaration of competing interest

The authors declare that they have no known competing financial interests or personal relationships that could have appeared to influence the work reported in this paper.

Acknowledgements

References

[1] B.L. Salvi, K.A. Subramanian, Sustainable development of road transportation sector using hydrogen energy system, Renew. Sustain. Energy Rev. 51 (2015) 1132–1155.
[2] J. Tollefson, COVID curbed carbon emissions in 2020—but not by much, Nature 589 (2021) 343.
[3] E. Commission, A Hydrogen Strategy for a Climate-Nuetral Europe. COM(2020), 2020, p. 301, final.
[4] R.S. El-Emam, H. Özcan, Comprehensive review on the techno-economics of sustainable large-scale clean hydrogen production, J. Clean. Prod. 220 (2019) 593–609.
[5] B. Zhang, S.-X. Zhang, R. Yao, Y.-H. Wu, J.-S. Qiu, Progress and prospects of hydrogen production: opportunities and challenges, Journal of Electronic Science and Technology 19 (2021) 100080.
[6] I. Dincer, C. Acar, Review and evaluation of hydrogen production methods for better sustainability, Int. J. Hydrogen Energy 40 (2015) 11094–11111.
[7] IEA. Global Hydrogen Review, 2021, p. 2021.
[8] M.R. Shaner, H.A. Atwater, N.S. Lewis, E.W. McFarland, A comparative technoeconomic analysis of renewable hydrogen production using solar energy, Energy Environ. Sci. 9 (2016) 2354–2371.
[9] T.T.Q. Vo, A. Xia, D.M. Wall, J.D. Murphy, Use of surplus wind electricity in Ireland to produce compressed renewable gaseous transport fuel through biological power to gas systems, Renew. Energy 105 (2017) 495–504.
[10] P. Nikolaidis, A. Poullikkas, A comparative overview of hydrogen production processes, Renew. Sustain. Energy Rev. 67 (2017) 597–611.
[11] F. Safari, I. Dincer, A review and comparative evaluation of thermochemical water splitting cycles for hydrogen production, Energy Convers. Manag. 205 (2020) 112182.
[12] F. Dawood, M. Anda, G.M. Shafiullah, Hydrogen production for energy: an overview, Int. J. Hydrogen Energy 45 (2020) 3847–3869.
[13] Y.A. Situmorang, Z. Zhao, A. Yoshida, A. Abudula, G. Guan, Small-scale biomass gasification systems for power generation (<200 kW class): a review, Renew. Sustain. Energy Rev. 117 (2020) 109486.
[14] M. van der Spek, C. Banet, C. Bauer, P. Gabrielli, W. Goldthorpe, M. Mazzotti, et al., Perspective on the hydrogen economy as a pathway to reach net-zero CO2 emissions in Europe, Energy Environ. Sci. 15 (2022) 1034–1077.
[15] V.S. Sikarwar, M. Zhao, P. Clough, J. Yao, X. Zhong, M.Z. Memon, et al., An overview of advances in biomass gasification, Energy Environ. Sci. 9 (2016) 2939–2977.
[16] S. Singla, N.P. Shetti, S. Basu, K. Mondal, T.M. Aminabhavi, Hydrogen production technologies-Membrane based separation, storage and challenges, J. Environ. Manag. (2022) 302.
[17] H. Ishaq, I. Dincer, Comparative assessment of renewable energy-based hydrogen production methods, Renew. Sustain. Energy Rev. 135 (2021) 110192.
[18] A. Hosseinzadeh, J.L. Zhou, X. Li, M. Afsari, A. Altaee, Techno-economic and environmental impact assessment of hydrogen production processes using bio-waste as renewable energy resource, Renew. Sustain. Energy Rev. 156 (2022) 111991.
[19] T. Terlouw, C. Bauer, R. McKenna, M. Mazzotti, Large-scale hydrogen production via water electrolysis: a techno-economic and environmental assessment, Energy Environ. Sci. 15 (2022) 3583–3602.
[20] Y.K. Salkuyeh, B.A. Saville, H.L. MacLean, Techno-economic analysis and life cycle assessment of hydrogen production from different biomass gasification processes, Int. J. Hydrogen Energy 43 (2018) 9514–9528.
[21] S. Chai, G. Zhang, G. Li, Y. Zhang, Industrial hydrogen production technology and development status in China: a review, Clean Technol. Environ. Policy 23 (2021) 1931–1946.
[22] A. Al-Sharafi, A.Z. Sahin, T. Ayar, B.S. Yilbas, Techno-economic analysis and optimization of solar and wind energy systems for power generation and hydrogen production in Saudi Arabia, Renew. Sustain. Energy Rev. 69 (2017) 33–49.
[23] H.A. Miller, K. Bouzek, J. Hnat, S. Loos, C.I. Bernäcker, T. Weißgärber, et al., Green hydrogen from anion exchange membrane water electrolysis: a review of recent developments in critical materials and operating conditions, Sustain. Energy Fuels 4 (2020) 2114–2133.
[24] I. Vincent, D. Bessarabov, Low cost hydrogen production by anion exchange membrane electrolysis: a review, Renew. Sustain. Energy Rev. 81 (2018) 1690–1704.
[25] I.V. Pushkareva, A.S. Pushkarev, S.A. Grigoriev, P. Modisha, D.G. Bessarabov, Comparative study of anion exchange membranes for low-cost water electrolysis, Int. J. Hydrogen Energy 45 (2020) 26070–26079.
[26] O. Schmidt, A. Gambhir, I. Staffell, A. Hawkes, J. Nelson, S. Few, Future cost and performance of water electrolysis: an expert elicitation study, Int. J. Hydrogen Energy 42 (2017) 30470–30492.
[27] D. Burnat, M. Schlupp, A. Wichser, B. Lothenbach, M. Gorbar, A. Züttel, et al., Composite membranes for alkaline electrolysis based on polysulfone and mineral fillers, J. Power Sources 291 (2015) 163–172.
[28] R. Phillips, W. Dunnill Charles, Zero gap alkaline electrolysis cell design for renewable energy storage as hydrogen gas, RSC Adv. 6 (2016) 100643–100651.
[29] T. Jordan, Chapter 2 - hydrogen technologies, in: A. Kotchourko, T. Jordan (Eds.), Hydrogen Safety for Energy Applications, Butterworth-Heinemann, 2022, pp. 25–115.
[30] J. Chi, H. Yu, Water electrolysis based on renewable energy for hydrogen production, Chin. J. Catal. 39 (2018) 390–394.
[31] M. Chatenet, B.G. Pollet, D.R. Dekel, F. Dionigi, J. Deseure, P. Millet, et al., Water Electrolysis: from Textbook Knowledge to the Latest Scientific Strategies and Industrial Developments, Chemical Society Reviews, 2022.
[32] L. Van Hoecke, L. Laffineur, R. Campe, P. Perreault, S.W. Verbruggen, S. Lenaerts, Challenges in the use of hydrogen for maritime applications, Energy Environ. Sci. 14 (2021) 815–843.
[33] D.D.A. de Fátima Palhares, L.G.M. Vieira, J.J.R. Damasceno, Hydrogen production by a low-cost electrolyzer developed through the combination of alkaline water electrolysis and solar energy use, Int. J. Hydrogen Energy 43 (2018) 4265–4275.
[34] S. Mazloomi, N. Sulaiman, Influencing factors of water electrolysis electrical efficiency, Renew. Sustain. Energy Rev. 16 (2012) 4257–4263.
[35] M.H. Sellami, K. Loudiyi, Electrolytes behavior during hydrogen production by solar energy, Renew. Sustain. Energy Rev. 70 (2017) 1331–1335.
[36] R.B. Slama, Hydrogen Production by Water Electrolysis Effects of the Electrodes Materials Nature on the Solar Water Electrolysis Performances, 2013.

[37] X. Zhang, S.H. Chan, H.K. Ho, S.-C. Tan, M. Li, G. Li, et al., Towards a smart energy network: the roles of fuel/electrolysis cells and technological perspectives, Int. J. Hydrogen Energy 40 (2015) 6866–6919.

[38] M. Lehner, R. Tichler, H. Steinmüller, M. Koppe, Power-to-gas: Technology and Business Models, Springer, 2014.

[39] M. Carmo, D.L. Fritz, J. Mergel, D. Stolten, A comprehensive review on PEM water electrolysis, Int. J. Hydrogen Energy 38 (2013) 4901–4934.

[40] S. Shiva Kumar, V. Himabindu, Hydrogen production by PEM water electrolysis – a review, Materials Science for Energy Technologies 2 (2019) 442–454.

[41] A. Godula-Jopek, Hydrogen Production: by Electrolysis, John Wiley & Sons, 2015.

[42] A.A. AlZahrani, I. Dincer, Modeling and performance optimization of a solid oxide electrolysis system for hydrogen production, Appl. Energy 225 (2018) 471–485.

[43] A. Nechache, S. Hody, Alternative and innovative solid oxide electrolysis cell materials: a short review, Renew. Sustain. Energy Rev. 149 (2021) 111322.

[44] A. Villagra, P. Millet, An analysis of PEM water electrolysis cells operating at elevated current densities, Int. J. Hydrogen Energy 44 (2019) 9708–9717.

[45] P.K.R. Holzapfel, M. Bühler, D. Escalera-López, M. Bierling, F.D. Speck, K.J.J. Mayrhofer, et al., Fabrication of a robust PEM water electrolyzer based on non-noble metal cathode catalyst: [Mo3S13]2− clusters anchored to N-doped carbon nanotubes, Small 16 (2020) 2003161.

[46] J. Mo, S. Wu, T.H.M. Lau, R. Kato, K. Suenaga, T.S. Wu, et al., Transition metal atom–doped monolayer MoS2 in a proton-exchange membrane electrolyzer, Materials Today Advances 6 (2020) 100020.

[47] S. Kasai, Hydrogen electrical energy storage by high-temperature steam electrolysis for next-millennium energy security, Int. J. Hydrogen Energy 39 (2014) 21358–21370.

[48] P. Moçoteguy, A. Brisse, A review and comprehensive analysis of degradation mechanisms of solid oxide electrolysis cells, Int. J. Hydrogen Energy 38 (2013) 15887–15902.

[49] A. Hauch, S.D. Ebbesen, S.H. Jensen, M. Mogensen, Highly efficient high temperature electrolysis, J. Mater. Chem. 18 (2008) 2331–2340.

[50] D. Simwonis, F. Tietz, D. Stöver, Nickel coarsening in annealed Ni/8YSZ anode substrates for solid oxide fuel cells, Solid State Ionics 132 (2000) 241–251.

[51] T. Nguyen, Z. Abdin, T. Holm, W. Mérida, Grid-connected hydrogen production via large-scale water electrolysis, Energy Convers. Manag. 200 (2019) 112108.

[52] H. Ju, S. Badwal, S. Giddey, A comprehensive review of carbon and hydrocarbon assisted water electrolysis for hydrogen production, Appl. Energy 231 (2018) 502–533.

[53] Fe Chakik, M. Kaddami, M. Mikou, Effect of operating parameters on hydrogen production by electrolysis of water, Int. J. Hydrogen Energy 42 (2017) 25550–25557.

[54] S. Wang, A. Lu, C.-J. Zhong, Hydrogen production from water electrolysis: role of catalysts, Nano Convergence 8 (2021) 4.

[55] N.A. Burton, R.V. Padilla, A. Rose, H. Habibullah, Increasing the efficiency of hydrogen production from solar powered water electrolysis, Renew. Sustain. Energy Rev. 135 (2021) 110255.

[56] J.A. Kilner, S. Skinner, S. Irvine, P. Edwards, Functional Materials for Sustainable Energy Applications, Elsevier, 2012.

[57] M. Chatenet, B.G. Pollet, D.R. Dekel, F. Dionigi, J. Deseure, P. Millet, et al., Water electrolysis: from textbook knowledge to the latest scientific strategies and industrial developments, Chem. Soc. Rev. 51 (2022) 4583–4762.

[58] K. Zeng, D. Zhang, Recent progress in alkaline water electrolysis for hydrogen production and applications, Prog. Energy Combust. Sci. 36 (2010) 307–326.

[59] L. Bertuccioli, A. Chan, D. Hart, F. Lehner, B. Madden, E. Standen, Study on Development of Water Electrolysis in the EU. Fuel Cells and Hydrogen Joint Undertaking, 2014, pp. 1–160.

[60] PIK. Price of hydrogen: data 12/04/2022. Available from: https://h2foroveralls.shinyapps.io/H2Dash/#section-visualisations (accessed 12/April/2022). 2022..

[61] D. Bogdanov, M. Ram, A. Aghahosseini, A. Gulagi, A.S. Oyewo, M. Child, et al., Low-cost renewable electricity as the key driver of the global energy transition towards sustainability, Energy 227 (2021) 120467.

[62] D. Gielen, R. Gorini, N. Wagner, R. Leme, L. Gutierrez, G. Prakash, et al., Global Energy Transformation: a Roadmap to 2050, 2019.

[63] I. Iea, World Energy Outlook 2017 Executive Summary. Energy Policy, 101016/0301-4215(73), 2017, 90024-4.

[64] (CEPCI) CEPCI. data 08/08/2022. Available from: https://www.toweringskills.com/financial-analysis/cost-indices/#cepci-2001-to-present (acccessed 8/August/2022). 2022..

[65] I. Dincer, Green methods for hydrogen production, Int. J. Hydrogen Energy 37 (2012) 1954–1971.

[66] R. Pinsky, P. Sabharwall, J. Hartvigsen, J. O'Brien, Comparative review of hydrogen production technologies for nuclear hybrid energy systems, Prog. Nucl. Energy 123 (2020) 103317.

[67] M. Al-Zareer, I. Dincer, M.A. Rosen, Performance analysis of a supercritical water-cooled nuclear reactor integrated with a combined cycle, a Cu-Cl thermochemical cycle and a hydrogen compression system, Appl. Energy 195 (2017) 646–658.

[68] C. Sattler, M. Roeb, C. Agrafiotis, D. Thomey, Solar hydrogen production via sulphur based thermochemical water-splitting, Sol. Energy 156 (2017) 30–47.

[69] J.H. Norman, J.L. Russell Jr., I.J.T. Porter, K.H. McCorkle, T.S. Roemer, R. Sharp, Process for the Thermochemical Production of Hydrogen, Google Patents, 1978.

[70] M. Sakurai, H. Nakajima, R. Amir, K. Onuki, S. Shimizu, Experimental study on side-reaction occurrence condition in the iodine–sulfur thermochemical hydrogen production process, Int. J. Hydrogen Energy 25 (2000) 613–619.

[71] M. Lo Faro, D.A. Cantane, F. Naro, In the path for creating Research-to-business new opportunities on green hydrogen between Italy and Brazil, Int. J. Hydrogen Energy (2022).

[72] G.F. Naterer, S. Suppiah, L. Stolberg, M. Lewis, Z. Wang, V. Daggupati, et al., Canada's program on nuclear hydrogen production and the thermochemical Cu–Cl cycle, Int. J. Hydrogen Energy 35 (2010) 10905–10926.

[73] Z. Ping, W. Laijun, C. Songzhe, X. Jingming, Progress of nuclear hydrogen production through the iodine–sulfur process in China, Renew. Sustain. Energy Rev. 81 (2018) 1802–1812.

[74] D. Scamman, M. Newborough, Using surplus nuclear power for hydrogen mobility and power-to-gas in France, Int. J. Hydrogen Energy 41 (2016) 10080–10089.

[75] Y. Lu, L. Zhu, C. Agrafiotis, J. Vieten, M. Roeb, C. Sattler, Solar fuels production: two-step thermochemical cycles with cerium-based oxides, Prog. Energy Combust. Sci. 75 (2019) 100785.

[76] C.N.R. Rao, S. Dey, Solar thermochemical splitting of water to generate hydrogen, Proc. Natl. Acad. Sci. USA 114 (2017) 13385–13393.

[77] M. Mehrpooya, B. Ghorbani, A. Ekrataleshian, S.A. Mousavi, Investigation of hydrogen production by sulfur-iodine thermochemical water splitting cycle using renewable energy source, Int. J. Energy Res. 45 (2021) 14845–14869.

[78] A. Singhania, Catalytic decomposition of hydrogen-iodide over nanocrystalline ceria promoted by transition metal oxides for hydrogen production in sulfur–iodine thermo-chemical cycle, Catal. Lett. 148 (2018) 1416–1422.

[79] Z. Ying, Y. Wang, X. Zheng, Z. Geng, B. Dou, G. Cui, Experimental study and development of an improved sulfur–iodine cycle integrated with HI electrolysis for hydrogen production, Int. J. Hydrogen Energy 45 (2020) 13176–13188.

[80] B.J. Lee, H.C. No, H.J. Yoon, S.J. Kim, E.S. Kim, An optimal operating window for the Bunsen process in the I–S thermochemical cycle, Int. J. Hydrogen Energy 33 (2008) 2200–2210.

[81] V.N. Ahmed, A.S. Rao, R. Sujeesh, H. Fani, A. Sanyal, S. Mukhopadhyay, Role of operating conditions on cross contamination of products of the Bunsen reaction in iodine-sulfur process for production of hydrogen, Int. J. Hydrogen Energy 42 (2017) 29101–29106.

[82] N. Li, P. Zhang, S. Chen, L. Wang, J. Xu, Study on apparent kinetics of the reaction between sulfuric and hydriodic acids in the iodine–sulfur process, Int. J. Chem. Kinet. 45 (2013) 588–595.

[83] R. Chaubey, S. Sahu, O.O. James, S. Maity, A review on development of industrial processes and emerging techniques for production of hydrogen from renewable and sustainable sources, Renew. Sustain. Energy Rev. 23 (2013) 443–462.

[84] G.F. Naterer, S. Suppiah, L. Stolberg, M. Lewis, Z. Wang, M. Rosen, et al., Progress in thermochemical hydrogen production with the copper–chlorine cycle, Int. J. Hydrogen Energy 40 (2015) 6283–6295.

[85] K. Pope, Z. Wang, G.F. Naterer, Process integration of material flows of copper chlorides in the thermochemical Cu–Cl cycle, Chem. Eng. Res. Des. 109 (2016) 273–281.

[86] S.E. Hosseini, M.A. Wahid, Hydrogen production from renewable and sustainable energy resources: promising green energy carrier for clean development, Renew. Sustain. Energy Rev. 57 (2016) 850–866.

[87] A. Farsi, I. Dincer, G.F. Naterer, Review and evaluation of clean hydrogen production by the copper–chlorine thermochemical cycle, J. Clean. Prod. 276 (2020) 123833.

[88] M.F. Orhan, I. Dincer, M.A. Rosen, Efficiency comparison of various design schemes for copper–chlorine (Cu–Cl) hydrogen production processes using Aspen Plus software, Energy Convers. Manag. 63 (2012) 70–86.

[89] A. Ozbilen, I. Dincer, M.A. Rosen, Life cycle assessment of hydrogen production via thermochemical water splitting using multi-step Cu–Cl cycles, J. Clean. Prod. 33 (2012) 202–216.

[90] S. Zhai, J. Rojas, N. Ahlborg, K. Lim, M.F. Toney, H. Jin, et al., The use of poly-cation oxides to lower the temperature of two-step thermochemical water splitting, Energy Environ. Sci. 11 (2018) 2172–2178.

[91] B.D. Ehrhart, C.L. Muhich, I. Al-Shankiti, A.W. Weimer, System efficiency for two-step metal oxide solar thermochemical hydrogen production – Part 1: thermodynamic model and impact of oxidation kinetics, Int. J. Hydrogen Energy 41 (2016) 19881–19893.

[92] A. Demont, S. Abanades, E. Beche, Investigation of perovskite structures as oxygen-exchange redox materials for hydrogen production from thermochemical two-step water-splitting cycles, J. Phys. Chem. C 118 (2014) 12682–12692.

[93] A. Bose, A. Farooqui, D. Ferrero, M. Santarelli, J. Llorca, Thermodynamic assessment of non-catalytic Ceria for syngas production by methane reduction and CO2 + H2O oxidation, Materials for Renewable and Sustainable Energy 8 (2019) 5.

[94] B.D. Ehrhart, C.L. Muhich, I. Al-Shankiti, A.W. Weimer, System efficiency for two-step metal oxide solar thermochemical hydrogen production – Part 3: various methods for achieving low oxygen partial pressures in the reduction reaction, Int. J. Hydrogen Energy 41 (2016) 19904–19914.

[95] S. Abanades, Metal oxides applied to thermochemical water-splitting for hydrogen production using concentrated solar energy, ChemEngineering 3 (2019).

[96] R.R. Bhosale, A. Kumar, P. Sutar, Thermodynamic analysis of solar driven SnO2/SnO based thermochemical water splitting cycle, Energy Convers. Manag. 135 (2017) 226–235.

[97] M. Chambon, S. Abanades, G. Flamant, Kinetic investigation of hydrogen generation from hydrolysis of SnO and Zn solar nanopowders, Int. J. Hydrogen Energy 34 (2009) 5326–5336.

[98] L. Arribas, J. González-Aguilar, M. Romero, Solar-driven thermochemical water-splitting by cerium oxide: determination of operational conditions in a directly irradiated fixed bed reactor, Energies 11 (2018).

[99] X. Huang, Z. Ruan, H. Zhang, Y. Yuan, Y. Shuai, Heat transfer analysis of thermal disassociation of ZnO for solar hydrogen production, Int. J. Hydrogen Energy 42 (2017) 18223–18231.

[100] R.R. Bhosale, Solar hydrogen production via ZnO/Zn based thermochemical water splitting cycle: effect of partial reduction of ZnO, Int. J. Hydrogen Energy 46 (2021) 4739–4748.

[101] E. Koepf, W. Villasmil, A. Meier, Pilot-scale solar reactor operation and characterization for fuel production via the Zn/ZnO thermochemical cycle, Appl. Energy 165 (2016) 1004–1023.

[102] Darfilal D. Solar hydrogen production by thermochemical reaction: development of a packed-bed reactor. J. Therm. Eng..6:152-169..

[103] R. Müller, A. Steinfeld, Band-approximated radiative heat transfer analysis of a solar chemical reactor for the thermal dissociation of zinc oxide, Sol. Energy 81 (2007) 1285–1294.

[104] A. Steinfeld, Solar hydrogen production via a two-step water-splitting thermochemical cycle based on Zn/ZnO redox reactions, Int. J. Hydrogen Energy 27 (2002) 611–619.

[105] A. Steinfeld, S. Sanders, R. Palumbo, Design aspects of solar thermochemical engineering—a case study: TWO-STEP WATER-SPLITTING CYCLE USING THE Fe3O4/FeO REDOX SYSTEM, Sol. Energy 65 (1999) 43–53.

[106] L. Wang, T. Ma, Z. Chang, H. Li, M. Fu, X. Li, Solar fuels production via two-step thermochemical cycle based on Fe3O4/Fe with methane reduction, Sol. Energy 177 (2019) 772–781.

[107] F. Safari, I. Dincer, A study on the Fe–Cl thermochemical water splitting cycle for hydrogen production, Int. J. Hydrogen Energy 45 (2020) 18867–18875.

[108] W.C. Chueh, C. Falter, M. Abbott, D. Scipio, P. Furler, S.M. Haile, et al., High-flux solar-driven thermochemical dissociation of CO2 and H2O using nonstoichiometric ceria, Science 330 (2010) 1797–1801.

[109] D. Arifin, A.W. Weimer, Kinetics and mechanism of solar-thermochemical H2 and CO production by oxidation of reduced CeO2, Sol. Energy 160 (2018) 178–185.

[110] B.J. Hathaway, R. Bala Chandran, A.C. Gladen, T.R. Chase, J.H. Davidson, Demonstration of a solar reactor for carbon dioxide splitting via the isothermal ceria redox cycle and practical implications, Energy & Fuels 30 (2016) 6654–6661.

[111] D. Marxer, P. Furler, M. Takacs, A. Steinfeld, Solar thermochemical splitting of CO2 into separate streams of CO and O2 with high selectivity, stability, conversion, and efficiency, Energy Environ. Sci. 10 (2017) 1142–1149.

[112] J.R. Scheffe, A. Steinfeld, Thermodynamic analysis of cerium-based oxides for solar thermochemical fuel production, Energy & Fuels 26 (2012) 1928–1936.

[113] S. Abanades, G. Flamant, Thermochemical hydrogen production from a two-step solar-driven water-splitting cycle based on cerium oxides, Sol. Energy 80 (2006) 1611–1623.

[114] L. Cao, K. Iris, X. Xiong, D.C. Tsang, S. Zhang, J.H. Clark, et al., Biorenewable hydrogen production through biomass gasification: a review and future prospects, Environ. Res. 186 (2020) 109547.

[115] L. Cao, I.K.M. Yu, X. Xiong, D.C.W. Tsang, S. Zhang, J.H. Clark, et al., Biorenewable hydrogen production through biomass gasification: a review and future prospects, Environ. Res. 186 (2020) 109547.

[116] V.S. Sikarwar, M. Zhao, P.S. Fennell, N. Shah, E.J. Anthony, Progress in biofuel production from gasification, Prog. Energy Combust. Sci. 61 (2017) 189–248.

[117] E. Shayan, V. Zare, I. Mirzaee, Hydrogen production from biomass gasification; a theoretical comparison of using different gasification agents, Energy Convers. Manag. 159 (2018) 30–41.

[118] D. Schweitzer, A. Gredinger, M. Schmid, G. Waizmann, M. Beirow, R. Spörl, et al., Steam gasification of wood pellets, sewage sludge and manure: gasification performance and concentration of impurities, Biomass Bioenergy 111 (2018) 308–319.

[119] S. Nanda, R. Rana, H.N. Hunter, Z. Fang, A.K. Dalai, J.A. Kozinski, Hydrothermal catalytic processing of waste cooking oil for hydrogen-rich syngas production, Chem. Eng. Sci. 195 (2019) 935–945.

[120] P. Parthasarathy, K.S. Narayanan, Hydrogen production from steam gasification of biomass: influence of process parameters on hydrogen yield – a review, Renew. Energy 66 (2014) 570–579.

[121] A. Molino, M. Migliori, A. Blasi, M. Davoli, T. Marino, S. Chianese, et al., Municipal waste leachate conversion via catalytic supercritical water gasification process, Fuel 206 (2017) 155–161.

[122] A.B.A. Ibrahim, H. Akilli, Supercritical water gasification of wastewater sludge for hydrogen production, Int. J. Hydrogen Energy 44 (2019) 10328–10349.

[123] M. Khadivi, T. Sowlati, Biomass Gasification Investment: a Multi-Criteria Decision Considering Uncertain Conditions, Biomass Conversion and Biorefinery, 2022.

[124] X. Xiong, I.K.M. Yu, L. Cao, D.C.W. Tsang, S. Zhang, Y.S. Ok, A review of biochar-based catalysts for chemical synthesis, biofuel production, and pollution control, Bioresour. Technol. 246 (2017) 254–270.

[125] F. Guo, Y. Dong, B. Tian, S. Du, S. Liang, N. Zhou, et al., Applications of microwave energy in gas production and tar removal during biomass gasification, Sustain. Energy Fuels 4 (2020) 5927–5946.

[126] J.A. Okolie, R. Rana, S. Nanda, A.K. Dalai, J.A. Kozinski, Supercritical water gasification of biomass: a state-of-the-art review of process parameters, reaction mechanisms and catalysis, Sustain. Energy Fuels 3 (2019) 578–598.

[127] Y.H. Chan, K.W. Cheah, B.S. How, A.C.M. Loy, M. Shahbaz, H.K.G. Singh, et al., An overview of biomass thermochemical conversion technologies in Malaysia, Sci. Total Environ. 680 (2019) 105–123.
[128] C. Gai, F. Zhang, T. Yang, Z. Liu, W. Jiao, N. Peng, et al., Hydrochar supported bimetallic Ni-Fe nanocatalysts with tailored composition, size and shape for improved biomass steam reforming performance, Green Chem. 20 (2018) 2788–2800.
[129] P. Gholkar, Y. Shastri, A. Tanksale, Catalytic reactive flash volatilisation of microalgae to produce hydrogen or methane-rich syngas, Appl. Catal. B Environ. 251 (2019) 326–334.
[130] N. Mahinpey, A. Gomez, Review of gasification fundamentals and new findings: reactors, feedstock, and kinetic studies, Chem. Eng. Sci. 148 (2016) 14–31.
[131] J. Dong, Y. Chi, Y. Tang, M. Ni, A. Nzihou, E. Weiss-Hortala, et al., Effect of operating parameters and moisture content on municipal solid waste pyrolysis and gasification, Energy & Fuels 30 (2016) 3994–4001.
[132] D.D.T. Ferraren-De Cagalitan, M.L.S. Abundo, A review of biohydrogen production technology for application towards hydrogen fuel cells, Renew. Sustain. Energy Rev. 151 (2021) 111413.
[133] L.S.F. Frowijn, W.G.J.H.M. van Sark, Analysis of photon-driven solar-to-hydrogen production methods in The Netherlands, Sustain. Energy Technol. Assessments 48 (2021) 101631.
[134] H. Argun, F. Kargi, Bio-hydrogen production by different operational modes of dark and photo-fermentation: an overview, Int. J. Hydrogen Energy 36 (2011) 7443–7459.
[135] Y.-C. Li, Y.-F. Liu, C.-Y. Chu, P.-L. Chang, C.-W. Hsu, P.-J. Lin, et al., Techno-economic evaluation of biohydrogen production from wastewater and agricultural waste, Int. J. Hydrogen Energy 37 (2012) 15704–15710.
[136] P. Mishra, S. Krishnan, S. Rana, L. Singh, M. Sakinah, Z. Ab Wahid, Outlook of fermentative hydrogen production techniques: an overview of dark, photo and integrated dark-photo fermentative approach to biomass, Energy Strategy Rev. 24 (2019) 27–37.
[137] M.L. Ghirardi, Implementation of photobiological H2 production: the O2 sensitivity of hydrogenases, Photosynth. Res. 125 (2015) 383–393.
[138] C. Ding, K.L. Yang, J. He, 11 - biological and fermentative production of hydrogen, in: R. Luque, C.S.K. Lin, K. Wilson, J. Clark (Eds.), Handbook of Biofuels Production, second ed., Woodhead Publishing, 2016, pp. 303–333.
[139] L. Ramanna, I. Rawat, F. Bux, Light enhancement strategies improve microalgal biomass productivity, Renew. Sustain. Energy Rev. 80 (2017) 765–773.
[140] D. Nagarajan, D.-J. Lee, A. Kondo, J.-S. Chang, Recent insights into biohydrogen production by microalgae – from biophotolysis to dark fermentation, Bioresour. Technol. 227 (2017) 373–387.
[141] Kumar S, Sharma S, Thakur S, Mishra T, Negi P, Mishra S, et al..
[142] A. Burlacot, G. Peltier, CHAPTER 8 Photosynthetic Electron Transfer Pathways during Hydrogen Photoproduction in Green Algae: Mechanisms and Limitations. Microalgal Hydrogen Production: Achievements and Perspectives, The Royal Society of Chemistry, 2018, pp. 189–212.
[143] Y. Shen, Carbon dioxide bio-fixation and wastewater treatment via algae photochemical synthesis for biofuels production, RSC Adv. 4 (2014) 49672–49722.
[144] R. Sivaramakrishnan, S. Shanmugam, M. Sekar, T. Mathimani, A. Incharoensakdi, S.-H. Kim, et al., Insights on biological hydrogen production routes and potential microorganisms for high hydrogen yield, Fuel 291 (2021) 120136.
[145] D.O. Corrêa, B. Santos, F.G. Dias, J.V.C. Vargas, A.B. Mariano, W. Balmant, et al., Enhanced biohydrogen production from microalgae by diesel engine hazardous emissions fixation, Int. J. Hydrogen Energy 42 (2017) 21463–21475.
[146] M.Y. Azwar, M.A. Hussain, A.K. Abdul-Wahab, Development of biohydrogen production by photobiological, fermentation and electrochemical processes: a review, Renew. Sustain. Energy Rev. 31 (2014) 158–173.
[147] B.D. Kossalbayev, T. Tomo, B.K. Zayadan, A.K. Sadvakasova, K. Bolatkhan, S. Alwasel, et al., Determination of the potential of cyanobacterial strains for hydrogen production, Int. J. Hydrogen Energy 45 (2020) 2627–2639.
[148] P. Sinha, A. Pandey, An evaluative report and challenges for fermentative biohydrogen production, Int. J. Hydrogen Energy 36 (2011) 7460–7478.
[149] R. Łukajtis, I. Hołowacz, K. Kucharska, M. Glinka, P. Rybarczyk, A. Przyjazny, et al., Hydrogen production from biomass using dark fermentation, Renew. Sustain. Energy Rev. 91 (2018) 665–694.
[150] E. Sağır, P.C. Hallenbeck, Chapter 6 - photofermentative hydrogen production, in: A. Pandey, S.V. Mohan, J.-S. Chang, P.C. Hallenbeck, C. Larroche (Eds.), Biohydrogen, second ed., Elsevier, 2019, pp. 141–157.
[151] A. Ghimire, L. Frunzo, F. Pirozzi, E. Trably, R. Escudie, P.N.L. Lens, et al., A review on dark fermentative biohydrogen production from organic biomass: process parameters and use of by-products, Appl. Energy 144 (2015) 73–95.
[152] J. Penniston, E.B. Gueguim Kana, Impact of medium pH regulation on biohydrogen production in dark fermentation process using suspended and immobilized microbial cells, Biotechnol. Biotechnol. Equip. 32 (2018) 204–212.
[153] Z.Y. Hitit, C.Z. Lazaro, P.C. Hallenbeck, Hydrogen production by co-cultures of Clostridium butyricum and Rhodopseudomonas palustris: optimization of yield using response surface methodology, Int. J. Hydrogen Energy 42 (2017) 6578–6589.
[154] K. Chandrasekhar, Y.-J. Lee, D.-W. Lee, Biohydrogen production: strategies to improve process efficiency through microbial routes, Int. J. Mol. Sci. 16 (2015).
[155] L. Singh, Z.A. Wahid, Methods for enhancing bio-hydrogen production from biological process: a review, J. Ind. Eng. Chem. 21 (2015) 70–80.
[156] J.-L. Fan, P. Yu, K. Li, M. Xu, X. Zhang, A levelized cost of hydrogen (LCOH) comparison of coal-to-hydrogen with CCS and water electrolysis powered by renewable energy in China, Energy 242 (2022) 123003.
[157] E.R.O. Zhiyuan Fan, Sarah Braverman, Yushan Laria Lou, Griffin Marie Smith, Green Hydrogen in a Circular Carbon Economy: Opportunities and Limits. Center on Global Energy Policy, Columbia SIPA, 2021.
[158] M.A. Adnan, M.G. Kibria, Comparative techno-economic and life-cycle assessment of power-to-methanol synthesis pathways, Appl. Energy 278 (2020) 115614.
[159] A. Khouya, Hydrogen production costs of a polymer electrolyte membrane electrolysis powered by a renewable hybrid system, Int. J. Hydrogen Energy 46 (2021) 14005–14023.
[160] A. Grimm, W.A. de Jong, G.J. Kramer, Renewable hydrogen production: a techno-economic comparison of photoelectrochemical cells and photovoltaic-electrolysis, Int. J. Hydrogen Energy 45 (2020) 22545–22555.
[161] N. Gerloff, Economic analysis of hydrogen production in Germany with a focus on green hydrogen, considering all three major water electrolysis technologies, Sustain. Energy Fuels 7 (2023) 1893–1907.
[162] E. Vartiainen, C. Breyer, D. Moser, E. Román Medina, C. Busto, G. Masson, et al., True cost of solar hydrogen, Sol. RRL 6 (2022) 2100487.
[163] H. Lee, B. Choe, B. Lee, J. Gu, H.-S. Cho, W. Won, et al., Outlook of industrial-scale green hydrogen production via a hybrid system of alkaline water electrolysis and energy storage system based on seasonal solar radiation, J. Clean. Prod. 377 (2022) 134210.
[164] J. Yates, R. Daiyan, R. Patterson, R. Egan, R. Amal, A. Ho-Baille, et al., Techno-economic analysis of hydrogen electrolysis from off-grid stand-alone photovoltaics incorporating uncertainty analysis, Cell Reports Physical Science 1 (2020) 100209.
[165] D. Jang, J. Kim, D. Kim, W.-B. Han, S. Kang, Techno-economic analysis and Monte Carlo simulation of green hydrogen production technology through various water electrolysis technologies, Energy Convers. Manag. 258 (2022) 115499.
[166] M. Minutillo, A. Perna, A. Forcina, S. Di Micco, E. Jannelli, Analyzing the levelized cost of hydrogen in refueling stations with on-site hydrogen production via water electrolysis in the Italian scenario, Int. J. Hydrogen Energy 46 (2021) 13667–13677.
[167] D. Schlund, M. Schönfisch, Analysing the impact of a renewable hydrogen quota on the European electricity and natural gas markets, Appl. Energy 304 (2021) 117666.
[168] J. Proost, State-of-the art CAPEX data for water electrolysers, and their impact on renewable hydrogen price settings, Int. J. Hydrogen Energy 44 (2019) 4406–4413.
[169] I.R.E.N.A. Renewables, Increasingly Beat Even Cheapest Coal Competitors on Cost, 2020.
[170] G. Glenk, S. Reichelstein, Economics of converting renewable power to hydrogen, Nat. Energy 4 (2019) 216–222.
[171] M. Tolga Balta, I. Dincer, A. Hepbasli, Thermodynamic assessment of geothermal energy use in hydrogen production, Int. J. Hydrogen Energy 34 (2009) 2925–2939.

[172] S. Sadeghi, S. Ghandehariun, A standalone solar thermochemical water splitting hydrogen plant with high-temperature molten salt: thermodynamic and economic analyses and multi-objective optimization, Energy 240 (2022) 122723.
[173] B. Parkinson, P. Balcombe, J.F. Speirs, A.D. Hawkes, K. Hellgardt, Levelized cost of CO2 mitigation from hydrogen production routes, Energy Environ. Sci. 12 (2019) 19–40.
[174] J. Kim, J. Park, Y.-S. Yoon, Simplified sulfur-iodine cycle process to hydrogen blast furnace: techno-economic and CO2 mitigation analysis, J. Clean. Prod. 355 (2022) 131855.
[175] S. Coulibaly, Y. Tang, S. Camara, J. Zhao, W. Li, A theoretical study of molten carbonate fuel cell combined with a solar power plant and Cu–Cl thermochemical cycle based on techno-economic analysis, Int. J. Hydrogen Energy 47 (2022) 22680–22690.
[176] M.I. Aydin, I. Dincer, An assessment study on various clean hydrogen production methods, Energy 245 (2022) 123090.
[177] S. Zhang, K. Li, P. Zhu, M. Dai, G. Liu, An efficient hydrogen production process using solar thermo-electrochemical water-splitting cycle and its techno-economic analyses and multi-objective optimization, Energy Convers. Manag. 266 (2022) 115859.
[178] J. Gorre, F. Ruoss, H. Karjunen, J. Schaffert, T. Tynjälä, Cost benefits of optimizing hydrogen storage and methanation capacities for Power-to-Gas plants in dynamic operation, Appl. Energy 257 (2020) 113967.
[179] L. Zhan, Y. Bo, T. Lin, Z. Fan, Development and outlook of advanced nuclear energy technology, Energy Strategy Rev. 34 (2021) 100630.
[180] H. Ding, W. Wu, D. Ding, Advancement of proton-conducting solid oxide fuel cells and solid oxide electrolysis cells at Idaho national laboratory (INL), ECS Trans. 91 (2019) 1029–1034.
[181] V. Pallozzi, A. Di Carlo, E. Bocci, M. Villarini, P.U. Foscolo, M. Carlini, Performance evaluation at different process parameters of an innovative prototype of biomass gasification system aimed to hydrogen production, Energy Convers. Manag. 130 (2016) 34–43.
[182] H.R. Sara, B. Enrico, V. Mauro, D.C. Andrea, N. Vincenzo, Techno-economic analysis of hydrogen production using biomass gasification -A small scale power plant study, Energy Proc. 101 (2016) 806–813.
[183] W. Han, Y.Y. Hu, S.Y. Li, F.F. Li, J.H. Tang, Biohydrogen production from waste bread in a continuous stirred tank reactor: a techno-economic analysis, Bioresour. Technol. 221 (2016) 318–323.
[184] W. Han, Z. Liu, J. Fang, J. Huang, H. Zhao, Y. Li, Techno-economic analysis of dark fermentative hydrogen production from molasses in a continuous mixed immobilized sludge reactor, J. Clean. Prod. 127 (2016) 567–572.
[185] W. Han, J. Fang, Z. Liu, J. Tang, Techno-economic evaluation of a combined bioprocess for fermentative hydrogen production from food waste, Bioresour. Technol. 202 (2016) 107–112.
[186] W. Han, Y. Yan, J. Gu, Y. Shi, J. Tang, Y. Li, Techno-economic analysis of a novel bioprocess combining solid state fermentation and dark fermentation for H2 production from food waste, Int. J. Hydrogen Energy 41 (2016) 22619–22625.
[187] M.F. Andrea, R.H. Sara, D.Z. Luca, S.S. Giovanni, B. Enrico, Techno-economic analysis of in-situ production by electrolysis, biomass gasification and delivery systems for Hydrogen Refuelling Stations: Rome case study, Energy Proc. 148 (2018) 82–89.
[188] C. Wulf, M. Kaltschmitt, Hydrogen Supply Chains for Mobility—Environmental and Economic Assessment. Sustainability, 2018.
[189] ISO 14040, Environmental Management-Life Cycle Assessment-Requirements and Guidelines; English Version, 2006. https://www.iso.org/standard/37456.html. (Accessed 16 May 2023).
[190] ISO 14044, Environmental Management-Life Cycle Assessment-Requirements and Guidelines; English Version, 2006. https://www.iso.org/standard/38498.html. (Accessed 16 May 2023).
[191] M. Delpierre, J. Quist, J. Mertens, A. Prieur-Vernat, S. Cucurachi, Assessing the environmental impacts of wind-based hydrogen production in The Netherlands using ex-ante LCA and scenarios analysis, J. Clean. Prod. 299 (2021) 126866.
[192] J. Zhang, B. Ling, Y. He, Y. Zhu, Z. Wang, Life cycle assessment of three types of hydrogen production methods using solar energy, Int. J. Hydrogen Energy 47 (2022) 14158–14168.
[193] R. Bhandari, C.A. Trudewind, P. Zapp, Life cycle assessment of hydrogen production via electrolysis – a review, J. Clean. Prod. 85 (2014) 151–163.
[194] J. Dufour, D.P. Serrano, J.L. Gálvez, J. Moreno, C. García, Life cycle assessment of processes for hydrogen production. Environmental feasibility and reduction of greenhouse gases emissions, Int. J. Hydrogen Energy 34 (2009) 1370–1376.
[195] Y. Khojasteh Salkuyeh, B.A. Saville, H.L. MacLean, Techno-economic analysis and life cycle assessment of hydrogen production from natural gas using current and emerging technologies, Int. J. Hydrogen Energy 42 (2017) 18894–18909.
[196] P.L.M.M. Spath, Life Cycle Assessment of Renewable Hydrogen Production via Natural Gas Steam Reforming and Wind Electrolysis, National Renewable Energy Laboratory, 2020.
[197] A. Ozbilen, I. Dincer, M.A. Rosen, A comparative life cycle analysis of hydrogen production via thermochemical water splitting using a Cu–Cl cycle, Int. J. Hydrogen Energy 36 (2011) 11321–11327.
[198] V. Utgikar, T. Thiesen, Life cycle assessment of high temperature electrolysis for hydrogen production via nuclear energy, Int. J. Hydrogen Energy 31 (2006) 939–944.
[199] A.E. Karaca, I. Dincer, J. Gu, Life cycle assessment study on nuclear based sustainable hydrogen production options, Int. J. Hydrogen Energy 45 (2020) 22148–22159.